

# Zonal vs. Nodal Pricing: An Analysis of Different Pricing Rules in the German Day-Ahead Market

Johannes Knörr<sup>a</sup>, Martin Bichler<sup>a</sup>, Teodora Dobos<sup>a,\*</sup>

<sup>a</sup>*School of Computation, Information and Technology, Technical University of Munich, Boltzmannstr. 3 Garching, 85748, Germany*

---

## Abstract

The European electricity market is based on large pricing zones with a uniform day-ahead price. The energy transition leads to changes in supply and demand and increasing redispatch costs. In an attempt to ensure efficient market clearing and congestion management, the EU Commission has mandated the Bidding Zone Review (BZR) to reevaluate the configuration of European bidding zones. Based on a unique data set published in the context of the BZR for the target year 2025, we compare the short-run effects of various pricing rules for the German power market. We compare market clearing and pricing for different zonal and nodal models, including their generation costs and associated redispatch costs. In numerical experiments with this dataset, the differences in the average prices in different zones are low. Congestion arises as well, but not necessarily on the cross-zonal interconnectors. The total costs across different configurations are similar and the reduction of standard deviations in prices is also small. This might be different with other load and generation scenarios, but the BZR data is important as it was created to make a decision about splits of the existing bidding zones. Nodal pricing rules lead to the lowest total cost. We also evaluate differences of nodal pricing rules with respect to the necessary uplift payments, which is relevant in the context of the current discussion on non-uniform pricing in the EU. While the study focuses on Germany, the analysis is relevant beyond and feeds into the broader discussion about pricing rules in non-convex markets.

*Keywords:* Nodal Pricing, Zonal Pricing, Non-Convex Markets, Redispatch

---

## 1. Introduction

A central discussion on electricity market pricing revolves around zonal and nodal pricing (aka. locational marginal pricing). Among the electricity wholesale markets implementing nodal pricing are Argentina, Chile, Mexico, New Zealand, Peru, Russia, Singapore, and several regions in the United States (U.S.). In contrast, a zonal pricing approach has been employed in the large and coupled EU market. Large groups of nodes are aggregated into zones, and the market clearing

---

\*Corresponding author

*Email addresses:* [knoerr@cit.tum.de](mailto:knoerr@cit.tum.de) (Johannes Knörr), [bichler@cit.tum.de](mailto:bichler@cit.tum.de) (Martin Bichler), [dobos@cit.tum.de](mailto:dobos@cit.tum.de) (Teodora Dobos)

problem only considers flow constraints between zones. It is supposed that no or only limited congestion occurs inside a zone. With some exceptions (e.g., Italy, Norway, Sweden), there is a single price zone within a country, and the day-ahead market provides a uniform national electricity price. Ignoring transmission constraints can lead to dispatch decisions that are not physically feasible. Thus, after the market clearing, transmission operators conduct redispatch to ensure that the final allocation aligns with physically feasible power flows. In the USA, all Independent System Operators (ISOs) moved from a zonal to a nodal model, partly due to steeply increasing redispatch costs. Aravena et al. (2021) provide an excellent summary of historical developments in different jurisdictions.

### *1.1. Zonal vs. Nodal Pricing*

Due to the ongoing energy transition, the zonal pricing paradigm has further come under scrutiny (Eicke & Schittekatte, 2022; Bertsch et al., 2016; Trepper et al., 2015a). Volatile renewable energy sources such as wind and solar lead to congestion in different parts of the electricity grid (Neuhoff et al., 2013). In addition, the energy transition can lead to structural problems. We will focus on Germany as a case in point. Energy is cleared as if there were no transmission constraints in Germany, but the traded energy can often not be delivered due to transmission constraints. As a result, redispatch volumes and costs have increased substantially in recent years to 34 TWh and EUR 3.1 billion in 2023 (Bundesnetzagentur, 2024). In an attempt to ensure efficient market clearing and congestion management, the EU Commission – as part of the Clean Energy Package – has mandated a Bidding Zone Review (BZR) to reevaluate the configuration of European bidding zones. An integral part of this process is a locational marginal pricing (LMP) study conducted by the European Network of Transmission System Operators for Electricity (ENTSO-E) as a basis to identify structural congestion and modified bidding zones. Having accurate data and grid models is central for the quality of the BZR. The LMP study constitutes the results of a multi-year effort of the European TSOs to provide a representative data set, and it is unparalleled in terms of the quality and degree of detail of the data. The study is based on an up-to-date model of the electricity grid and supply and demand estimates for 2025 and different climate scenarios. In this study, ENTSO-E solved linearized unit commitment models with marginal pricing to obtain nodal prices (ENTSO-E, 2022). Based on the resulting prices, in August 2022, the European Union Agency for the Cooperation of Energy Regulators (ACER) decided on a set of alternative bidding zone configurations (ACER, 2022a). Following Article 16 of the BZR methodology, ENTSO-E has published non-confidential data related to the LMP study (ENTSO-E, 2023). We refer to this data set as the BZR data in what follows and leverage this dataset to expand on the results of the LMP study, focusing on the German bidding zone. Germany is particularly interesting, because ACER suggested the evaluation of several configurations with splits of the large German-Luxembourgish bidding zone.

## 1.2. Challenges in Congestion Management

A key driver of the BZR is ensuring efficient congestion management. Congestion occurs when transmission capacity is insufficient to accommodate the flow of electricity from generation units to demand centers, leading to bottlenecks that require operational adjustments like redispatch or curtailment. Over the last years, redispatch costs and curtailment rates have increased considerably in Europe due to the increasing integration of variable renewable energy sources (VRE), limited storage capabilities and insufficient transmission capacity. In 2024, the European Commission proposed an emissions reduction of 90% by 2040 compared to the 1990 levels (European Commission, 2024). This objective depends on the deployment of renewable sources. Current efforts primarily focus on installing renewable capacity in areas with the highest resource potential and overlook the grid topology and the local demand. Regions rich in renewable generation potential may not align with areas of high electricity demand. Thus, the need to transmit power within zones could frequently surpass the capacity of the grid, leading to congestion and increased curtailment of renewable generation. Newbery (2023) and Newbery & Biggar (2024) discuss the inefficiency of current European market designs from the perspective of the VRE merchants, emphasizing that investments are driven by average curtailment rates, which fail to account for significantly higher marginal curtailment rates.<sup>1</sup> This misalignment risks promoting overinvestment in poorly connected areas, since, according to the authors, marginal curtailment is more than three times higher than average curtailment. A recent study by Thomassen et al. (2024) suggests that in a grid expansion scenario that extrapolates current trends, up to 310 TWh of renewable generation could be curtailed in 2040 due to the limitations in the grid. Moreover, even in an extreme grid expansion scenario that involves expanding the length of the European grid by more than a third, the total redispatch volumes would increase almost sixfold compared to 2022. While the increase in curtailment rates and redispatch volumes is predictable, addressing these challenges requires a thorough evaluation of alternative market designs and pricing techniques.

## 1.3. Related Literature

A few recent studies aimed to analyze the impact of a bidding zone split on Germany or other countries in Europe. These studies are typically based on proprietary data sets and models and they assume different target years. The consulting company Aurora published results of another study where they predict 5 Euros per MWh price difference between the north and the south of Germany in the years 2030, increasing to 9 Euros in 2045.<sup>2</sup> Models and data are proprietary. In another study by the EWI and THEMA consulting<sup>3</sup> the authors predict differences in prices in a southern and a northern zone of around 15 to 10 Euros per MWh between 2024 and 2033, with a decreasing trend. The study is based on two separate models and data by the EWI and THEMA

---

<sup>1</sup>Marginal curtailment represents the extra curtailment caused by the last MW of capacity installed. Average curtailment is defined as the total curtailed volume divided by the total installed capacity.

<sup>2</sup><https://auroraer.com/insight/power-market-impact-of-splitting-the-german-bidding-zone/>

<sup>3</sup><https://www.ewi.uni-koeln.de/en/publications/price-impact-of-a-german-bidding-zone-split/>

consulting that are not publicly available. The size of the spread differs in THEMA’s and EWI’s results according to the authors. For 2030 the study makes a number of assumptions regarding electrolysers and new lines being built, batteries, and a shift of renewables from North to South. Tiedemann et al. (2024) discuss the market value of renewable energy sources after a zonal split for 2030. Their study is based on a data set and grid model by the Fraunhofer IEE and they predict around 10 Euros per MWh difference between the north and south of Germany respectively in 2030. They do not comment on reductions in redispatch by a zonal split.

It is worth mentioning that the data sets used in these studies and the underlying grid models differ substantially, and so do the target years analyzed. For example, there are differences in the number of lines in the BZR data set compared to the widely used JAO Static Grid model.<sup>4</sup> Also, the assumptions made for supply and demand for the future differ. We stick to the BZR dataset which appears to have a very comprehensive grid model and a near-term target year of 2025.<sup>5</sup> Moreover, the redispatch methods used in these studies might be different. The study by EWI and THEMA, while not disclosing the specific implementation details, calculated redispatch volumes using a “*using a welfare optimal redispatch procedure with limited countertrading*”. The study by Aurora does not disclose any details regarding how redispatch is computed.

In November 2024, ENTSO-E published the absolute average market prices for the alternative configurations (ENTSO-E, 2024). According to ENTSO-E, for the scenario year 2009 (see Section 2.2), a two-zone split leads to an absolute average price of 45.05 EUR/MWh in the North and 49.81 EUR/MWh in the South, which is equivalent to a 4.77 EUR/MWh price difference between the zones. Averaging over all three years considered in the LMP Study, the absolute average prices observed in the North and in the South differ by approximately 7 EUR/MWh. We note that these results were computed in a study that considers the whole Bidding Zone Review “Central Europe”. As outlined in Section 1.5, our market clearing problem includes only Germany and does not incorporate any neighboring countries. The results published by ENTSO-E also suggest that a two, three or four-zone split of Germany leads to price increases in most of the Central European countries.

All of the previously mentioned studies analyze *static* models where demand and supply are given as we do. Ambrosius et al. (2020) use a multi-level mixed-integer non-linear model based on Grimm et al. (2019) to analyze investment incentives over time. Such models cannot accommodate the level of detail in static models due to their computational complexity, such that the paper is based on an aggregation of the German electricity network into 28 nodes. However, the approach complements static models taking into account the long-run effects of prices on investment. Several articles discuss the impact of price splits on transmission and generation investment incentives and

---

<sup>4</sup>JAO Static Grid model contains 837 lines at or above the 220kV voltage level (see <https://www.jao.eu/static-grid-model>, accessed in May 2024). The dataset we use consists of 2407 lines spanning various voltage levels, both below and above 220kV (see Section 2.2).

<sup>5</sup>There are also earlier studies on a zonal split, such as those by Trepper et al. (2015a), but the data sets and assumptions are even harder to compare due to the significant changes in the past ten years.

emission reductions (Grimm et al., 2016, 2021, 2022). For example, Grimm et al. (2021) predict that a split of the German market into two price zones has only a small impact on efficiency. Considering 3 grid expansion scenarios to be implemented by 2040, Thomassen et al. (2024) analyze the evolution of redispatch costs for a large part of the EU based on a model consisting of 1024 nodes. Their study is built upon the PyPSA-Eur framework (Hörsch et al., 2018) and shows that the redispatch volumes and costs will increase substantially regardless of the grid expansion scenario. For instance, in the extreme grid expansion scenario that the authors analyze, which implies enlarging the total grid length of Europe by more than a third, the redispatch volumes increase almost sixfold. Several studies, focusing on various jurisdictions, estimate the static dispatch inefficiencies of a zonal market design to range between 0.5% and 3% (Simshauser, 2025; Holmberg & Tangerås, 2023; Green, 2007; Leuthold et al., 2008; Aravena & Papavasiliou, 2016).

Another stream in the literature asks how zones should be split. While some papers focus on identifying configurations by clustering power transfer distribution factors (PTDFs) (e.g., (Kumar et al., 2004) and (Kłos et al., 2014)), most works use LMPs as clustering features (Stoft, 1997). Burstedde (2012) computes LMPs for the scenario years 2015 and 2020 considering a simplified 72-node representation of the European grid, and evaluates the shapes and sizes of the zones obtained by clustering these LMPs using hierarchical clustering. Breuer et al. (2013) implement a genetic algorithm and apply it on a dataset consisting of 380 kV nodes considering a projected system for 2016 and 2018. Based on six scenarios, Felling & Weber (2018) compute robust price zone configurations for Central Western Europe by employing hierarchical clustering based on the LMPs of approximately 2,200 nodes and assigning weights to nodes depending on their demand- and supply situation. Dobos et al. (2025) use the BZR data and the published nodal prices to compute zones with low price variance. They show that the clusterings they found are not robust across time or the clustering method used. These studies use heuristics to identify price zone configurations. In contrast, Grimm et al. (2019) propose a mixed-integer nonlinear model to divide a market area into a specific number of price zones, ensuring the resulting configuration is welfare-optimal. Ambrosius et al. (2020) extend this model by including capacity investment decisions, aiming to determine both the optimal price zone configuration and the available transfer capacities between zones.

Finally, there is an extensive literature on nodal pricing and different pricing rules to deal with the non-convexities of power markets. We refer the interested reader to Liberopoulos & Andrianesis (2016) for an excellent overview. The most prominent examples of nodal pricing rules are Integer Programming (IP) pricing (O’Neill et al., 2005) and Convex Hull (CH) pricing (Gribik et al., 2007; Hogan & Ring, 2003; Bichler et al., 2022). Both are used in a number of U.S. markets (MISO, 2023; PJM, 2018). Both pricing rules require side-payments by the market operator to compensate losses of market participants (make-whole payments, MWPs) or even to compensate all incentives to deviate from the efficient allocation (lost opportunity costs, LOCs). These pricing rules are now being discussed in Europe in the context of non-uniform pricing rules. In particular, Pollitt (2023) analyzes whether and how nodal prices should be implemented in Europe. CH pricing is known to provide poor congestion signals. We also draw on a recent proposal by Ahunbay et al. (2024) that

trades off make-whole payments and the quality of the congestion signal and evaluate these three pricing rules in the context of our study, which provides input for the discussion on non-uniform pricing in the EU day-ahead market (All NEMO Committee, 2023).

#### 1.4. Contributions

Our goal is to understand how prices in these configurations compare to nodal prices and the current market design with a uniform national price. Specifically, we compare the total costs and prices that arise for national, zonal, and different nodal models. For this we leverage the BZR data set, which provides the most comprehensive and most recent data set available about the European power grid and serves as a foundation for decisions by EU authorities.

In contrast to earlier studies, the average price differences across zonal configurations between 1 and 4 zones for Germany are low, less than 3.5 EUR/MWh. There are also individual days where the price difference between zones is more than 10 EUR/MWh, but on average the differences are small.<sup>6</sup> For the scenarios in the BZR data with climate year 2009, the excess supply in the north of Germany after computing a nodal dispatch was typically such that the cross-zonal lines or interconnectors were not a binding constraint. There was congestion in the network, but not necessarily on the interconnectors.<sup>7</sup> This finding extends to differences in the redispatch between different zonal configurations. It is difficult to model real-world redispatch practices of TSOs. We could only implement two simplified minimal-cost and minimal-volume redispatch methods. Real-world practices are more complicated, but we argue that it provides a reasonable approximation for redispatch costs. While these redispatch costs decrease slightly from one to two zones, we see little effect with further splits. The cross-zonal capacities play a role for these differences and we will discuss them in more detail below. Our findings do not mean that there cannot be scenarios of supply and demand in Germany where cross-zonal links become binding and there are differences in prices. However, in the BZR dataset, intended to inform ACER and other stakeholders, this is not what we find.

The BZR dataset also provides us with an opportunity for an apples-to-apples comparison of zonal and nodal pricing rules. So, we can quantify the effect of moving from a zonal to a nodal pricing regime. In our study, nodal prices lead to higher generation costs than zonal pricing, but to lower total costs taking our estimated redispatch costs into account. This is due to the fact that redispatch is largely avoided in nodal pricing systems. However, there are different ways how nodal prices can be computed and these nodal pricing rules are currently being discussed in the context of the new capacity management rules CACM 2.0 (All NEMO Committee, 2023). In other words, the comparison between nodal and zonal prices also depends on the nodal pricing rule. We consider Integer Programming (IP) pricing (O’Neill et al., 2005) (as used in U.S. power markets)

---

<sup>6</sup>In 2018, the Austria was split from the joint price zone with Germany. Demand and supply is significantly different between both countries, yet prices (after the gas crises in 2021 and 22) are often remarkably close as well (see <https://www.energy-charts.info/>).

<sup>7</sup>We do not model critical elements within zones, but we reduce the available capacity on the interconnectors to account for such elements (Section 2.1.2).

and Convex Hull (CH) pricing (Hogan & Ring, 2003; Gribik et al., 2007) as two established pricing rules in U.S. markets, and the recently proposed Join pricing rule (Ahunbay et al., 2024). We also implement a simplified version of Euphemia (NEMO Committee, 2024). The results illustrate the trade-offs that can be expected in terms of quality of the congestion signals and minimum make-whole payments.<sup>8</sup> While our analysis focuses on Germany, the policy implications of our study go beyond in that they analyze the differences between different zonal and nodal pricing rules based on a realistic dataset.

### 1.5. Limitations

Like any model-based analysis of its kind, also our study makes assumptions and faces some limitations. *First*, a central assumption that all such studies need to make for a split of the price zone are the cross-zonal line capacities. Transmission capacity allocation in the field is a complex task with several decisions made by TSOs, that cannot easily be predicted and modeled (see Section 2.1.2). In line with earlier studies (see Section 2.1.2 for a discussion), we compute market clearing solutions in which only 80% of the transmission line limits are considered to take into account security considerations. With higher security margins there might be higher differences in the prices between zones. *Second*, as in any simulation, the way how we compute redispatch can only be an approximation of real-world practices, which are complex (see decision BK8-18-0007-A by the German Bundesnetzagentur). For example, we do not provide a detailed accounting of curtailment costs. We also assume that every generator can be redispatched, but this is not the case in reality. So, the computed redispatch costs serve only as an approximation, but we argue that it provides a fair comparison. *Third*, our examination focuses on the German day-ahead market without incorporating neighboring countries, cross-border trades, or loop flows through other countries. We do incorporate 100 neighboring nodes not in Germany though to mitigate the effect and argue that the consideration of more nodes outside Germany will not lead to higher differences in the prices between zones in Germany but rather the opposite. However, flows from neighboring countries – which we do not include in our analysis – could enhance congestion and, thus, lead to higher redispatch volumes and costs in Germany. *Fourth*, we do not consider the long-run effects of the prices and congestion management regime corresponding to specific market clearing models. While this paper focuses on short-run inefficiencies, long-run inefficiencies – such as suboptimal location choices and technology decisions for generation and consumption – are also crucial factors to consider when evaluating a market clearing model. *Fifth*, we assume fixed, inelastic demand from the ENTSO-E dataset<sup>9</sup>, neglecting the potential for demand response under nodal prices. Incentives for demand response would be in favor of nodal pricing rules. Moreover, we assume that the demand

---

<sup>8</sup>We compared the nodal prices that we computed to those published in the BZR dataset. The latter were based on duals of a linear programming relaxation of entire European dispatch problem. Details of this model have not been released but the average nodal prices that we computed are not significantly different to those published in the BZR dataset in a sample of hourly prices analyzed.

<sup>9</sup>In European electricity markets, demand is inelastic and must be satisfied in any feasible market-clearing solution (NEMO Committee, 2024).

cannot be redispatched, as it is current practice in Germany. *Sixth*, the current European market is characterized by portfolio bidding, differing from the unit-commitment bids underlying both the study by ENTSO-E and our analysis. Portfolio bids allow optimization of trades across assets and differ from those feasible in nodal market designs. Incorporating such considerations into our analysis would require making strong and potentially unwarranted assumptions regarding market participant behavior. Neither the LMP study nor we make such assumptions. *Seventh*, as any other study of this sort, we do not model the intraday or forward markets. *Finally*, the data set provided by ENTSO-E was constructed for the target year 2025, and it is important to acknowledge that analyses can vary based on differing assumptions regarding supply and demand. However, the ENTSO-E dataset represents the best source available today for such a study. The assumptions made for our analysis are described in Section 2.2.

We also want to emphasize that the discussion surrounding zonal and nodal pricing extends beyond dispatch and prices. In the ongoing Bidding Zone Review, a comprehensive approach is adopted which considers factors such as liquidity, security of supply, transition costs, and investments in low-carbon technologies, which we can not replicate in our analysis.

### 1.6. Organization

The remainder of this article is structured as follows. In Section 2.1, we introduce our unit commitment model and formalize nodal and zonal market clearing. We also review the IP, CH, and Join pricing rules. Section 2.2 elaborates on the data sources used to implement our dispatch model and outlines our experimental design. Section 3 presents the key results of our analysis of different market clearing and pricing rules. Lastly, Section 4 provides a summary and conclusions.

## 2. Methods

### 2.1. Clearing and Pricing on Electricity Markets

#### 2.1.1. Preliminaries

We consider an electricity market consisting of a set of buyers  $B$  and a set of sellers  $S$ , each located at nodes  $N$  in an interconnected electricity network. The set of power lines  $L$  is encoded as pairs of nodes  $(n, m)$ , and we consider multiple periods  $T$ . An item in this market corresponds to a unit of electricity at a particular node  $n \in N$  at a specific time  $t \in T$ .

A buyer  $b \in B$  possesses a valuation function  $v_b : \mathbb{R}^{N \times T} \rightarrow \mathbb{R}$  that quantifies the buyer’s preferences and constraints. We consider inelastic demand, hence the valuation function simplifies to strict demand satisfaction. Similarly, a seller  $s \in S$  has a cost function  $c_s : \mathbb{R}^{N \times T} \rightarrow \mathbb{R}$ .

The market operator collects these buy and sell bids to calculate a feasible allocation. As electricity is transmitted over the network, the allocation is subject to physical power flows, encoded as a constraint set  $\Psi$ . An accurate representation of the transmission network would require  $\Psi$  to be equivalent to AC optimal power flow (ACOPF) constraints (Molzahn & Hiskens, 2019). However, it is well known that the ACOPF is intractable for realistic problem sizes, and electricity market operators need to employ computationally scalable approximations of the ACOPF.



### 2.1.2. Market Clearing

In practice, market operators employ different bidding languages to encode  $v_b$  and  $c_s$ , as well as different approximations  $\Psi$  of the power flow constraints. In this work, we use the data released for the European bidding zone review to compare allocation and prices under different market clearing mechanisms.

In full generality, the market operator seeks an allocation  $(x, y)$ , where  $x = (x_b)_{b \in B}$ ,  $x_b \in \mathbb{R}^{N \times T}$  is the allocation vector of buyers and  $y = (y_s)_{s \in S}$ ,  $y_s \in \mathbb{R}^{N \times T}$  is the allocation vector of sellers. The market operator identifies an allocation that maximizes welfare, by solving the following optimization model:

$$\begin{aligned} \max_{x,y} \quad & \sum_{b \in B} v_b(x_b) - \sum_{s \in S} c_s(y_s) \\ \text{subject to} \quad & x, y \in \Psi. \end{aligned} \tag{1}$$

On European day-ahead markets, buyers and sellers submit hourly bids and block orders (NEMO Committee, 2019). The BZR data, however, does not contain bids of this structure. Instead, it provides generator and load characteristics similar to unit commitment problems in U.S. markets. Specifically, for a buyer  $b$  located in a node  $n_b$ <sup>10</sup> there is only information on a fixed demand profile  $P_b \in \mathbb{R}^{N \times T}$ , while price-elastic bids are unavailable. Consequently, the valuation function of  $b$  simplifies to strict demand satisfaction.

$$v_b(x_b) = \begin{cases} -\infty, & x_b \neq P_b \\ 0, & x_b = P_b \end{cases} \tag{2}$$

For sellers/generators  $s \in S$ , the BZR data release includes more detailed information. Each generator  $s$  has a minimum and maximum production quantity  $\underline{P}_s \in \mathbb{R}$  and  $\bar{P}_s \in \mathbb{R}$  at their node  $n_s$ . Moreover, once a generator has been started, there is a minimum uptime constraint to run for at least  $\underline{R}_s \in \mathbb{Z}_0^+$  periods. Generators incur variable costs  $g_s$  to produce electricity and fixed costs  $h_s$  whenever the generator runs. We use a binary commitment variable  $u_{st} \in \{0, 1\}$  to model a

---

<sup>10</sup>For  $t \in T, n \in N \setminus \{n_b\}, x_{b,nt} = 0$ .

generator's constraint set  $P_s$ .

$$\begin{aligned}
P_s = \{y_s \in \mathbb{R}^{N \times T} : & y_{s,n_st} \geq \underline{P}_{st} u_{st} & \forall t \in T, \\
& y_{s,n_st} \leq \overline{P}_{st} u_{st} & \forall t \in T, \\
& \phi_{st} \geq u_{st} - u_{s(t-1)} & \forall t \in T \setminus \{T_0\}, \\
& \sum_{i=t-\underline{R}_s+1}^t \phi_{si} \leq u_{st} & \forall t \in T \setminus \{T_0\}, \\
& y_{s,nt} = 0 & \forall n \in N \setminus \{n_s\}, t \in T \\
& u_{st} \in \{0, 1\} & \forall s \in S, t \in T. \}
\end{aligned}$$

With this constraint set, we define a generator's cost function  $c_s$  as follows.

$$c_s(y_s) = \begin{cases} \infty, & y_s \notin P_s \\ \sum_{t \in T} g_s y_{s,n_st} + \sum_{t \in T} h_s u_{st}, & y_s \in P_s \end{cases} \quad (3)$$

Given that only price-inelastic demand bids are available, the objective of problem (1) can be interpreted as minimizing generators' costs required to fulfill the demand.

During the 2000s and 2010s, many U.S. ISO markets moved from zonal to nodal pricing. Recognizing that an accurate representation of the transmission network in the form of the ACOPF is computationally infeasible, market operators resort to linearized versions of power flow. The most common implementation is the Direct Current OPF (DCOPF), which is based on three simplifying assumptions (Stott et al., 2009; Molzahn & Hiskens, 2019), i.e., (1) uniform voltage magnitudes, (2) negligibly small voltage angle differences, and (3) neglecting line resistances and reactive power. Under these assumptions, the flow constraints can be expressed as simple linear constraints:

$$\Psi^{DC} = \{(x, y, \theta) : \sum_{s \in S} y_{s,nt} - \sum_{b \in B} x_{b,nt} = \sum_{m \in N} -B_{nm}(\theta_{nt} - \theta_{mt}) \forall n \in N, t \in T\} \quad (4)$$

In (4),  $B_{nm}$  is the susceptance of the line connecting nodes  $n$  and  $m$ . The voltage angle decision variable for node  $n$  and period  $t$  is denoted as  $\theta_{nt}$ . If such a line does not exist, then  $B_{nm} = 0$ , and  $B_{nn} = 0 \forall n$ . The constraint set in (4) can be enriched by further constraints, such as box constraints on the voltage angles, and more (Li et al., 2022). We use such a standard DCOPF model in our analysis, similar to what was used in the ENTSO-E study. Note that this representation of the DCOPF using line susceptances is equivalent to the representation that considers PTDFs. When the representation  $\Psi$  of the transmission network includes all nodes in the transmission network, we refer to nodal market clearing. When only a subset of the grid is considered, we speak of zonal market clearing, as discussed in the following. Power system operators need to consider contingencies for a secure operation of the network. The system should satisfy the  $(N - 1)$  criterion to guarantee that the power system is operated safely in the normal condition or in any contingency case (Christie et al., 2000; Marien et al., 2013; Weinhold & Mieth, 2024). Rather than a

full security-constrained optimal power flow (SCOPF) model (Hinojosa, 2020), we consider a safety margin of 20% on all transmission lines. Appendix A includes a compact formulation of the nodal market clearing problem.

### *Zonal Market Clearing*

The key idea of zonal pricing is to aggregate nodes into zones and only consider transmission flows across zones. This simplifies the constraint set  $\Psi$  significantly, enhances computational scalability, and allows for portfolio bidding of larger market participants. An important parameter of a zonal power system is the determination of the capacities of interconnectors between the zones.

In the European market, two approaches have been implemented: the net transfer capacity (NTC) model and the flow-based market coupling (FBMC) methodology (NEMO Committee, 2019). FBMC was introduced in Central Western Europe in 2015 and has since been extended to neighboring markets. In FMBC, the net export possible from one zone to another is limited by the remaining available margin (RAM) on the critical network elements connecting the zones. The RAM is determined by the maximum allowable flow (e.g., thermal capacity) subtracting the physical flow before the optimization (the base case), and a flow reliability margin to cover uncertainty in the capacity and allocation computations (Marien et al., 2013; Weinhold & Mieth, 2024). The Flow-Based Market Coupling with Generation Shift Keys (FBMC-GSK) is the specific methodology currently being used in the EU. The way how the interconnection capacity between two price zones is calculated and allocated in FBMC-GSK depends on how various parameters are set and the critical network elements considered by the TSOs (Aravena et al., 2021), and cannot be predicted precisely for an eventual split of the German price zone. Furthermore, the FBMC approach necessitates access to a PTDF matrix that indicates how zone net position changes affect cross-zonal flows. Such a PTDF matrix is not included in the BZR data.

In our zonal market clearing implementation, we consider all interconnectors as critical network elements and model their physical characteristics via the DCOPF constraints (4). In line with earlier literature (Tiedemann et al., 2024; Wyrwoll et al., 2018; Voswinkel et al., 2019), we compute a base case that only takes 80% of the capacities of all interconnectors into account. Similar to the nodal model, this should take into account the  $(N - 1)$  security criterion (Christie et al., 2000). The zonal flow constraints can be written as:

$$\Psi^{Zonal} = \{(x, y, \theta) : \sum_{s \in S} y_{s,zt} - \sum_{b \in B} x_{b,zt} = \sum_{n \in z, m \notin z} -B_{nm}(\theta_{nt} - \theta_{mt}) \forall z \in Z, t \in T\} \quad (5)$$

We denote by  $(x^{Zonal}, y^{Zonal}, \theta^{Zonal})$  a day-ahead spot market solution that satisfies the zonal flow constraints. The mapping of nodes to zones is suggested by the ENTSO-E study on locational marginal pricing (ACER, 2022b). Four different zonal splits were proposed for the German bidding zone, suggesting between two to four price zones. The first two constraints in Appendix A can be easily adapted based on equation (5) to obtain the zonal market clearing problem that we consider.

### *Redispatch*

While zonal market clearing is computationally less expensive than nodal market clearing, it

substantially simplifies the underlying physical power flows. In fact, the economic outcome of zonal market clearing is usually infeasible with physical power flows. As a result, transmission operators resort to *redispatch*, i.e., modifying the economic allocation to provide a physically feasible outcome.

In the Single Day-Ahead Coupling Region (SDAC), the economic allocation is determined using the Euphemia algorithm (NEMO Committee, 2024). This allocation includes decisions on order acceptance and power flows between the bidding zones. The allocation results are published around 12:30 CET<sup>11</sup>, setting fixed day-ahead schedules. After these results are released, redispatch begins, which occurs during the period leading up to real-time delivery.

Current redispatch mechanisms consider two paradigms: Firstly, cost-based redispatch, as implemented in Germany, reimburses redispatched generators for their additional costs or lost profits and makes them indifferent to the previous market outcome. Secondly, market-based redispatch aims at a bid-based procurement of redispatch volumes. Market-based redispatch was criticized as prone to market power abuse and causing inc-dec gaming, i.e., strategic bidding in day-ahead markets to generate higher profits in subsequent redispatch markets (Hirth & Schlecht, 2020).

The precise redispatch methodology implemented by TSOs is not publicly disclosed. While Article 35 of the CACM Regulation states that “*Each TSO shall coordinate the use of redispatching and countertrading resources, taking into account their impact on operational security and economic efficiency*”, it does not detail the coordination process or provide formal definitions of operational security and economic efficiency. The German legislation (§13 EnWG) states that “*In the case of power and voltage-related adjustments to active power generation or active power consumption [...], among several suitable measures [...], those measures are to be selected which are expected to cause the lowest overall costs*”. However, the legislation does not provide the mathematically precise definition that has to be considered by TSOs. There are several studies that touch upon redispatch computation and employ different models. Ambrosius et al. (2022); Grimm et al. (2019) and Trepper et al. (2015b) consider a redispatch problem that has as objective minimizing the cost difference between the redispatch and the spot (zonal) solutions. Moreover, Kunz & Zerrahn (2015) consider a model that minimizes the sum of redispatch costs, costs associated with load shedding and costs associated with renewable generation curtailment.

In this paper, we consider three redispatch methods which have the same constraints but different objective functions. We assume that demand cannot be redispatched, as it is current practice in Germany. This means that the (inelastic) demand  $P_b$  for all  $b \in B$  will be fully satisfied both in the zonal and in the redispatch solution.

*RD-Min-Cost:* The first method is a simplified cost-based redispatch that computes a modified allocation which satisfies the constraint set of  $\Psi^{DC}$  while minimizing the redispatch costs. Let  $R$  denote the set of renewables,  $Cur^{res}$  the quantity of renewable generation curtailment corresponding to  $res \in R$  and  $c_{cur}$  the curtailment cost per MW. Given the outcome of the zonal allocation

---

<sup>11</sup>The order book closes at 12:00 CET and then Euphemia computes a solution within 12 minutes.

$(x^{Zonal}, y^{Zonal}, \theta^{Zonal})$ , we consider the following problem:

$$\begin{aligned} \min_{x,y,\theta} \quad & \sum_{s \in S} c_s (y_s - y_s^{Zonal}) + \sum_{res \in R} c_{cur} Cur^{res} \\ \text{subject to} \quad & x = x^{Zonal} \\ & (x, y, \theta) \in \Psi^{DC} \end{aligned} \tag{6}$$

Negative (positive) redispatch occurs when  $y_s < y_s^{Zonal}$  ( $y_s > y_s^{Zonal}$ ). Negative redispatch implies cost savings since generation costs are avoided, which leads to a decrease in the overall redispatch costs. These costs must be reimbursed by power plants to TSOs. Positive redispatch requires additional generation costs for upward production, causing an increase in the total redispatch costs. This method ensures that the cheap (expensive) generators are selected for upward (downward) redispatch. Note that it also assumes that every generator can be redispatched, which might not be the case in practice.<sup>12</sup> We assume that the set of renewables  $R$  includes offshore wind, onshore wind and photovoltaic units. The curtailment costs are set to the variable costs presented in Table B.20, which reflect the variable and annual operating costs.<sup>13</sup>

*RD-Min-Comp*: The second method minimizes the compensations paid to sellers for their adjustments in generation. These compensations are provided for both upward and downward redispatch and are computed based on the cost curve of each generator according to the following objective:

$$\min_{x,y,\theta} \sum_{s \in S} c_s |y_s - y_s^{Zonal}| \tag{7}$$

*RD-Min-Vol*: The third method minimizes the redispatch volumes:

$$\min_{x,y,\theta} \sum_{s \in S} |y_s - y_s^{Zonal}| \tag{8}$$

The objective value of each method represents the total redispatch costs associated with it. A redispatch solution is interpreted as the final DCOPF-feasible allocation  $(x, y, \theta)$  that can be implemented as physical power flows. Note that a DCOPF-feasible solution may still be ACOPF-infeasible and require further adjustments to the allocation, which we disregard in this work. Market participants subject to redispatch must be compensated for lost profits, reducing overall welfare. In our numerical experiments, we thus consider *system costs* as the total cost of generation *before*

---

<sup>12</sup>Until 2021, only production units with a capacity of at least 10 MW could be redispatched. The Grid Expansion Acceleration Act (Netzausbaubeschleunigungsgesetz, NABEG 2.0) introduced the current system, Redispatch 2.0, in which units with a capacity of at least 100 kW can be redispatched. Redispatch 3.0, currently under discussion, aims to further extend it by integrating units with capacities below 100 kW. This would allow for redispatch of all production units, aligning with the method that we implement in this study.

<sup>13</sup>Since the curtailment costs are meant to cover the lost revenue plus additional expenses incurred by curtailed renewable units, the costs from Table B.20 act as a lower bound for the actual curtailment costs.

redispatch, *redispatch costs* themselves, and *total costs* as the sum of system and redispatch costs.

### 2.1.3. Pricing on Non-Convex Markets

Once an allocation  $(x, y)$  has been obtained, the market operator must provide electricity prices  $p \in \mathbb{R}^{N \times T}$  for each node and time period. Due to the non-convexities implied by sellers' cost functions (i.e., the binary commitment variables  $u_{st}$ ), this is not a trivial task. In microeconomics, the *welfare theorems* provide a foundation for pricing in markets. In their seminal paper, Arrow & Debreu (1954) demonstrate that under convex preferences, demand independence, and perfect competition with divisible items, a market operator can always achieve a set of Walrasian equilibrium prices that support the welfare-maximizing allocation. We assume *quasilinear* utilities, i.e., the utility of each market participant is defined as the difference between valuation or costs and price.

$$\begin{aligned} u_b(x|p) &= v_b(x) - \sum_{n \in N, t \in T} p_{nt} x_{b,nt} \quad \forall b \in B \\ u_s(y|p) &= \sum_{n \in N, t \in T} p_{nt} y_{s,nt} - c_s(y) \quad \forall s \in S \end{aligned} \quad (9)$$

At given prices  $p$ , each market participant has some preferred bundles that maximize utility. We call these bundles the *demand set* and denote the maximum possible utility as follows.

$$\begin{aligned} \hat{u}_b(p) &= \max_x v_b(x) - \sum_{n \in N, t \in T} p_{nt} x_{b,nt} \quad \forall b \in B \\ \hat{u}_s(p) &= \max_y \sum_{n \in N, t \in T} p_{nt} y_{s,nt} - c_s(y) \quad \forall s \in S. \end{aligned} \quad (10)$$

A Walrasian equilibrium consists of a market-clearing allocation and linear prices such that no participant has an incentive to deviate.

**Definition 1** (Walrasian Equilibrium). *A price vector  $p$  and a feasible allocation  $(x, y)$  form a Walrasian equilibrium if:*

1. (*Market clearing*) *Supply equals demand, i.e.,  $\sum_{s \in S, n \in N} y_{s,nt} = \sum_{b \in B, n \in N} x_{b,nt} \forall t \in T$ .*
2. (*Envy-freeness*) *Every market participant maximizes their utility at the prices, i.e.,  $u_b(x|p) = \hat{u}_b(p) \forall b \in B$  and  $u_s(y|p) = \hat{u}_s(p) \forall s \in S$ .*
3. (*Budget balance*) *The payments that sellers receive equal the payments that buyers provide, i.e.,  $\sum_{n \in N, t \in T} p_{nt} (\sum_{s \in S} y_{s,nt} - \sum_{b \in B} x_{b,nt}) = 0$ .*

Unfortunately, real-world electricity markets do not satisfy the assumptions underlying the welfare theorems. As in many other markets, items are not perfectly divisible and market participants exhibit non-convex preferences. A large stream of literature has investigated existence conditions for Walrasian equilibria in non-convex markets (Kelso & Crawford, 1982; Bikhchandani & Ostroy, 2002; Baldwin & Klemperer, 2019), but none of these conditions are satisfied in electricity markets.

Bikhchandani & Mamer (1997) demonstrate that Walrasian equilibria exist if and only if the linear relaxation of the allocation problem has an integer solution. When this is not the case, market participants bear (global) *lost opportunity costs* at any set of prices and do not maximize their individual profits, violating envy-freeness.

Consequently, market operators have to resort to heuristic pricing rules that aim at approximating Walrasian equilibrium prices. Many such pricing rules have been proposed (Liberopoulos & Andrianesis, 2016), each compromising on the properties of Walrasian equilibria differently. In this work, we focus on *Convex Hull* (CH) pricing (Hogan & Ring, 2003; Gribik et al., 2007) as two established pricing rules in practice, as well as on the *Join* pricing rule (Ahunbay et al., 2024) as a novel multi-objective approach to pricing. We also consider the *Euphemia* pricing rule as it is applied in European electricity markets.

#### *Convex Hull Pricing*

In the absence of Walrasian equilibrium prices, there is no set of prices  $p$  that maximizes the profit of every market participant. The concept of global lost opportunity costs describes this forgone payoff.

**Definition 2** (Global Lost Opportunity Costs (GLOCs)). *Given an allocation  $(x, y)$  and prices  $p$ , a market participant's global lost opportunity costs describe the difference between their individual payoff maximum, given  $p$ , and their actual payoff.*

$$\begin{aligned} GLOC_b &= \hat{u}_b(p) - u_b(x|p) \\ GLOC_s &= \hat{u}_s(p) - u_s(y|p) \end{aligned}$$

The key idea of CH (Convex Hull) pricing (Hogan & Ring, 2003; Gribik et al., 2007) is to minimize GLOCs over all market participants. Formally, CH pricing replaces each non-convex cost function  $c_s(y_s)$  with its convex envelope in (1), and derives prices from the dual of the resulting convex problem.

Computing convex envelopes and determining CH prices is generally computationally challenging (Schiro et al., 2016). However, it has been shown by Hua & Baldick (2017) that CH pricing becomes tractable when the cost function is described as in (3). Specifically, by relaxing the binary constraints  $u_{st} \in \{0, 1\}$  to  $u_{st} \in [0, 1]$  and solving the dual of (1), CH prices can be obtained from a single linear program. This approach, also referred to as Extended Locational Marginal Pricing (ELMP), was also used by the recent ENTSO-E study (ENTSO-E, 2022).

#### *IP Pricing*

In a convex market, Walrasian equilibrium prices are equivalent to *marginal* prices, i.e., the costs of the last accepted bid set the prices. Following this notion, O'Neill et al. (2005) try to generalize marginal pricing for non-convex markets. Their IP (Integer Programming) pricing rule assumes that generators cannot easily deviate from their commitment status (as encoded by the binary variable  $u_{st}$ ) and sets prices equal to the variable costs of the marginal *committed* unit (i.e., the marginal unit among all units with  $u_{st} = 1$ ).

IP pricing has gained popularity in many practical markets. It involves three steps: (i) obtaining the optimal commitment variables  $u_{st}^*$  from the allocation problem in (1), (ii) fixing the commitment variables of each generator to these optimal values, i.e., setting  $u_{st} \in \{0, 1\}$  to  $u_{st} \in [0, 1]$  with  $u_{st} = u_{st}^*$  in (3), and (iii) solving (1) with these linearized cost functions and extracting prices from its dual.

IP prices can be considered Walrasian equilibrium prices assuming that no generator can deviate from its commitment status. In other words, every participant maximizes their utility *locally*, meaning under fixed commitment. We define these *local lost opportunity costs* a subset of GLOCs.

**Definition 3** (Local Lost Opportunity Costs (LLOCs)). *Given an allocation  $(x, y)$ , generator commitments  $u^*$ , and prices  $p$ , a seller's local lost opportunity costs describe the difference between their individual payoff maximum under fixed commitment, given  $p$ , and their actual payoff.*

$$LLOC_s = \hat{u}'_s(p) - u_s(y|p) \text{ with } \hat{u}'_s(p) = \hat{u}_s(p) \text{ s.t. } u = u^*$$

By convexity of  $v_b(x_b)$ , a buyer's LLOCs exactly equal their GLOCs. Besides computational tractability, IP prices accurately reflect the marginal value of transmission capacity (Yang et al., 2019). Specifically, price differences among nodes arise solely when the network experiences congestion. It has been shown that this property immediately corresponds minimizing LLOCs (Ahunbay et al., 2024), making them a significant indicator of good *congestion signals*.

#### *Join Pricing*

In most electricity markets, neither GLOCs nor LLOCs are paid out to market participants to disincentivize deviations from the optimal allocation. Instead, market operators merely ensure that no participant incurs losses by participating in the market, ensuring non-negative utilities and, equivalently, *individual rationality*. The payments to ensure individual rationality are known as *make-whole payments*.

**Definition 4** (Make-Whole Payments (MWP)). *Given an allocation  $(x, y)$  and prices  $p$ , a market participant's make-whole payments describe their negative payoff, if applicable.*

$$MWP_b = \max\{-u_b(x|p), 0\}$$

$$MWP_s = \max\{-u_s(y|p), 0\}$$

Bids that require MWPs are also known as *paradoxically accepted bids*. MWPs can be regarded as another subset of GLOCs, referring only to participants' incentives to not participate in the market at all. However, both CH and IP pricing can experience high levels of MWPs. Recent practical concerns have thus motivated the development of pricing rules that ensure lower levels of MWPs. Among them is the Join pricing rule (Ahunbay et al., 2024), which proposes a dual pricing problem that combines the objective of IP pricing (minimizing LLOCs) with minimizing MWPs. Specifically, for each participant it considers the maximum of LLOCs and MWPs in the objective, leading to a robust and computationally tractable pricing rule with adequate congestion signals



and low MWPs simultaneously.

In US electricity markets, MWPs are generally not covered directly by revenues obtained from the buyers through energy purchases in the day-ahead market but require additional funding mechanisms which depend on the ISO (Townsend et al., 2014).<sup>14</sup> ISOs often impose uplift charges or ancillary service fees on market participants to fund MWPs. These charges are ultimately passed on to electricity consumers, either directly through consumption fees or indirectly through higher electricity bills.

#### 2.1.4. *Euphemia*

CH, IP, and Join pricing all have in common that they price the welfare-maximizing allocation. Market participants incur lost opportunity costs; some are even paradoxically accepted and need to be compensated by MWPs.

European electricity markets follow a different approach. Paradoxically accepted bids are not permitted, and instead, the market operator deviates from the welfare-maximizing outcome to avoid paying any MWPs. This is the essence of the *Euphemia* day-ahead clearing algorithm (NEMO Committee, 2019). Note that avoiding paradoxically accepted bids does not satisfy the envy-freeness property from Definition 1. Market participants still incur GLOCs and LLOCs, a subset of which are even rejected to participate in the market even though it would be profitable for them to do so. Such bids are referred to as *paradoxically rejected bids*.

The *Euphemia* algorithm combines market clearing and pricing (unlike the pricing rules above which can be applied to any pre-computed allocation). In European markets, it computes an allocation and *zonal* prices, but theoretically, it can also be applied in nodal markets. Algorithmically, it starts by computing the welfare-maximizing allocation, solving (1). It then advances to examining whether prices can be established for the allocation, i.e., they must prevent any paradoxically accepted bids, ensure the acceptance of all in-the-money hourly bids and, optionally, certify that cross-zonal flows occur from a lower-price to a higher-price zone. If paradoxically accepted bids exist, *Euphemia* adds cuts to (1) that eliminate the current candidate solution, constraining the allocation problem and leading to welfare losses. These iterations between allocation and pricing continue until a solution without paradoxically accepted bids is reached.

Subsequently, *Euphemia* continues by addressing some of the idiosyncrasies of the European market (PUN search, re-insertion of certain paradoxically rejected bids, resolving indeterminacy). If, at any of these steps, violations are detected, the iterative procedure continues. Eventually, *Euphemia* outputs allocation, zonal prices, and cross-zonal flows.

Since we aim to investigate prices and welfare losses associated with *Euphemia*, we implemented a simplified version of the algorithm for our numerical experiments. With the data provided, however, we can only replicate the first two steps of the algorithm, i.e., the iterative allocation and pricing procedure. When a paradoxically accepted seller  $s$  in period  $t$  is detected, we add a

---

<sup>14</sup>MWPs are also referred to as bid productions cost guarantees (NYISO), revenue sufficiency guarantees (MISO) and operating reserve credits (PJM).

constraint  $u_{st} = 0$  to the allocation problem (1). No open-source implementation of the algorithm is available, but we followed the public description as closely as possible.

A practical problem with Euphemia is its computational tractability. Due to its iterative nature, multiple mixed-integer problems must be solved until allocation and prices are obtained. With the planned 15-min market time unit introduction in Europe, the scalability of Euphemia poses a significant concern, and policymakers consider non-uniform pricing rules (such as the ones introduced above) to obtain solutions faster (All NEMO Committee, 2022).

## 2.2. Data and Processing

This study examines welfare, prices, and GLOCs, LLOCs and MWP for multiple zonal/nodal configurations, allocation rules, and pricing mechanisms. As discussed, we leverage the data released in the context of the European bidding zone review (ENTSO-E, 2022; ACER, 2022b). We focus on Germany as arguably one of the most important bidding zones regarding clearing volume and its central position in the European grid. In this section, we provide an overview of the data set and our processing of it.

### 2.2.1. Bidding Zone Review Data

In September 2022, ENTSO-E, on behalf of all European TSOs, released various data sets related to their locational pricing study (ENTSO-E, 2022, 2023). The input data structure along two primary datasets: the *grid model* as a basis for the transmission network and the *input files* to model generation and demand. Data on reserves, storage, and imports/exports were not considered in our study. Along with these input data, results files such as locational prices and cleared generation, demand, and storage were released. The publication refers to a total of 24 weeks over three representative climate years (1989, 1995, and 2009). Only the climate information from 1989, 1995, and 2009 is used, while generation and demand scenarios were generated for the target year 2025 (ENTSO-E, 2022).

Unfortunately, some parts of the data were aggregated before their publication (e.g., local demand to country-wide demand), and some data were not revealed (e.g., a mapping of generators in the *input files* to their location in the *grid model*). Without access to these proprietary data, the outcome of the ENTSO-E study cannot be exactly reproduced. However, we could assign most of generators to locations via OpenStreetMap.<sup>15</sup>

Let us discuss the data in more depth. The topology of the grid, defined by its nodes and connections, dictates the paths electricity takes from generation to consumption, with substations facilitating the necessary voltage transformations along the way. Substations act as critical nodes in the network that manage voltage levels for efficient power flow. A substation might handle multiple voltage levels. For example, a transmission substation might receive power at a very high voltage (e.g., 220kV or higher) and step it down to a lower high voltage (e.g., 110kV) for further transmission or to a medium voltage (e.g., 10-35kV) for distribution to urban or industrial areas.

---

<sup>15</sup><https://www.openstreetmap.de/>

The ENTSO-E dataset provides a model of Germany’s power grid, detailing 834 substations. Each of these substations encompasses one or more voltage levels, summing up to 1697 voltage levels at substations in the dataset. These voltage levels cover the spectrum from transmission ( $\geq 220\text{kV}$ ) to distribution ( $\leq 110\text{kV}$ ) and are composed of several topological nodes. Altogether, there are 2898 topological nodes listed in the data sets. Additionally, the dataset includes details for 100 substations located in the neighboring countries, which have been integrated into our analysis. For our study, we manually determined the geographical locations of all substations and computed prices for all voltage levels on these substations. After some pre-processing, which involved removing disconnected nodes, breakers, and disconnectors, our German grid model consists of 1670 nodes and 2407 lines (Schmitt, 2023). Technically, supply and demand on different voltage levels of substations do not necessarily need to be the same. However, it turned out that prices computed for voltage levels on a substation were identical or very close in the ENTSO-E dataset, which is also the case for the nodal prices provided by ENTSO-E. Overall, the average prices that we computed were not significantly different from those in the BZR dataset for substations. There were differences on individual nodes, which is probably due to the fact that the prices computed by ENTSO-E are based on the duals of a linear programming relaxation, while we use the mixed integer linear program and pricing rules as they are defined above.

For the grid constraints of our DCOPF in (4), we derive the per-unit susceptance  $B_{nm}$  for each line from the given actual susceptance and base admittance (Grainger & Stevenson, 1994). We also induce transmission limits on each power line, which we infer as the minimum of each line’s angular stability limit (inferred from its surge impedance loading and the St. Clair curve (St. Clair, 1953)), voltage drop limit (inferred from voltage and reactance (Hao & Xu, 2008)), and thermal limit (inferred from voltage and current on a three-phase system (Moreira et al., 2006)). We assume these transmission limits to be constant over time. Missing data, e.g., on the length and susceptance of lines, were replaced by the data in the JAO Static Grid Model where possible, and else inferred from the mean of all other lines. As discussed earlier, we reserved a buffer of 20% on the transmission limits to account for secure operations of the electricity grid.

For the demand side, the *input files* provide hourly aggregated load profiles for the entire country of Germany. Neither the nodal distribution of demand nor demand valuations are provided. Demand-side response was considered in the ENTSO-E study, but no related data was released. We distributed demand proportional to each consumer’s base load that is available as part of the *grid model*. We thereby assume that demand fluctuations over time occur uniformly across all consumers (Schmitt, 2023). We further assume that demand is price-inelastic, as was done in the study by ENTSO-E.

The *input files* pertaining to the supply side are more granular and separated by generator type, i.e., Hard Coal, Lignite, Gas, Light Oil, Solar, Hydro Run-Of-River, Hydro Reservoir, Hydro PumpOL, Hydro PumpCL, Onshore Wind, Offshore Wind, Other Non-RES, and Other RES. They contain operational characteristics of thermal units, derived from the Pan-European Market Modeling Database (PEMMDB), and hourly aggregated output of renewable energy sources,

derived from Pan European Climate Database (PECD). The operational characteristics include – among others – minimum / maximum power and minimum runtime requirements that we use to parameterize our generator cost functions. The data also includes must-run obligations, start-up / shut-down times, and ramp rates, which may be used to further extend the model. Similarly, data on storage or demand response could leverage more detailed models.

As the maximum power of each seller is given as a fixed quantity (denoting its nominal capacity), we need to manually incorporate the variability of renewable energy sources. We thus distribute the aggregate dispatched energy in each hour equally to all plants of the same type, proportional to their nominal capacities, and set the maximum power to this value. The underlying assumptions are that renewables are always dispatched at maximum power and that meteorological conditions are equal across Germany. Because hydro power plants are dispatchable, they are excluded from this logic. Out of 4537 generation units that we consider, 1709 ( $\approx 37\%$ ) are subject to unit-commitment rigidities. These units have minimum uptime and minimum operating power requirements greater than 0. The data also do not include information on variable or fixed costs for renewables, which we derived from literature (Kost et al., 2021; IRENA, 2022; ENTSO-E, 2022). For thermal units, variable cost information are provided, while fixed cost information were again obtained from literature (Kost et al., 2021; Schröder et al., 2013; Bundesnetzagentur, 2022). We refer the reader to Appendix B for more details.

An additional challenge is the mapping of generators to corresponding network nodes. The grid data specify the broad category of generating units at each node (e.g., thermal, hydro, external injections) and their nominal capacities. While renewable resources could be mapped to the seller data by matching nominal capacities, the grid data lacks additional information regarding thermal plant types. We assigned thermal generators in the grid to their operational characteristics (such as minimum uptime constraints) (Schmitt, 2023). Firstly, we match identifiers with the *Kraftwerksliste* (power plant list) provided by the Bundesnetzagentur to obtain each generator’s broad thermal generation type (e.g., lignite, gas, etc.). As nominal capacities do not match between grid and seller data, and seller data have a higher granularity (e.g., Gas CCGT, Gas OCGT, etc.), we solve an integer program to assign each entity in the grid model to exactly one corresponding seller of the same plant type, with the objective to minimize the aggregated differences in capacities and number of units per plant type. We provide this integer program and the outcome of the generation matching in Appendix C. While this assignment might not be exact, we argue that smaller mistakes in the assignment of generators to nodes have little impact on the more general questions raised in our paper that address the benefits of different zonal and nodal configurations. The data are accessible through the ENTSO-E website.

Importantly, the data we use in our study reflects the target year 2025, while the fraction of the generator types is expected to change as Germany continues its energy transition (Energiewende) toward a greener power supply. According to the (Federal Ministry of Education and Research, 2024), renewable energy sources are projected to account for up to 80% of gross electricity consumption by 2050. In addition, coal-fired power plants are set to be completely phased out by 2038

(The Federal Government, 2024), while the share of combined-cycle gas turbine (CCGT) plants is expected to increase temporarily to compensate for the reduction in coal and to support the intermittent nature of renewable energy sources.

### 2.2.2. Experimental Design

We implemented the models in Python 3.11 using Gurobi to solve optimization problems. We conducted experiments for eight weeks in 2009, as suggested by the ENTSO-E report (ENTSO-E, 2022), for the German bidding zone. To maintain computational feasibility of calculating hourly allocations and prices, we permitted a MIP gap of 5% for mixed-integer programs. Table 1 summarizes our experimental design and the scope of our analysis.

We first employ different allocation rules in accordance with the ENTSO-E report. These configurations range from a national single-zone model to a fully nodal model, as well as the ACER proposals for two to four bidding zones ACER (2022b). Each allocation is associated with generation costs as well as redispatch costs to obtain a physically feasible outcome. After computing an allocation, different pricing rules, such as IP, CH, or Join pricing, can be applied. Each pricing rule implies different price levels as well as MWPs for market participants. Prices were capped at 100 EUR/MWh to limit the impact of outliers. Note that prices higher than 100 EUR/MWh are regarded as outliers also in the BZR Report (Section 2.4) (ENTSO-E, 2022). We also consider the Euphemia allocation and prices as the current implementation in European markets.

Calendar Weeks of 2009	Allocation Rules	Pricing Rules	Focus Variables
04	National	IP	Generation Costs
08	2 Zones (k-means)	CH	Redispatch Costs
11	2 Zones (spectral)	Join	Prices
15	3 Zones		MWPs
16	4 Zones		
21	Nodal		
31	Euphemia		
48			

Table 1: Overview of experiments

## 3. Results

In this section, we summarize the main results of our analysis. We start with comparing average generation and total costs, before discussing price levels and MWPs. We report aggregate statistics for all weeks under consideration and further pick the days of February 18, March 10, and November 23 for an in-depth analysis of representative days with low, medium, and high prices, respectively.

### 3.1. Generation and Redispatch Costs

Table 2 presents an overview of the average daily generation and redispatch costs, calculated using the RD-Min-Cost redispatch method described in Section 2.1.2, for the allocation rules under consideration. The table also includes the total generation and redispatch costs. Additional

results computed with the other redispatch methods are provided in Appendix D Table 3 shows the percentage decrease of the nodal costs relative to the total costs associated with different zonal configurations.<sup>16</sup>

in kEUR	National	2 Zones (k)	2 Zones (s)	3 Zones	4 Zones	Nodal
Generation	33,507.00	33,702.87	33,697.10	33,578.77	33,717.41	36,150.7
RD-Min-Cost	5,491.06	5,195.02	5,238.15	5,438.16	5,264.69	0
Total RD-Min-Cost	38,998.06	38,897.89	38,935.25	39,016.93	38,982.1	36,150.7

Table 2: Average Daily Costs

%	National	2 Zones (k)	2 Zones (s)	3 Zones	4 Zones
Total RD-Min-Cost	7.88	7.6	7.7	7.93	7.83

Table 3: Percentage decrease of the nodal costs relative to the total costs associated with different zonal configurations

The numbers reported in Table 2 have realistic orders of magnitude as compared to those provided by the German Bundesnetzagentur (Bundesnetzagentur, 2024). However, our goal is not to come up with a precise prediction of costs for 2025, but to obtain a relative comparison between different zonal configurations and nodal pricing. Adding network constraints cannot lead to lower objective function values in the cost minimization. As the national allocation rule neglects all transmission constraints, their generation costs are a lower bound for all other allocation rules. On average, the suggested zonal configurations require only slightly more generation costs, suggesting that adding few transmission constraints to the computation has little impact on the costs. In contrast, the nodal allocation rule includes the entire transmission network. Obviously, higher generation costs are required to reach an allocation with feasible power flows. On average, generation costs increase by 7.88% after including all network constraints for the nodal model compared to the national configuration before redispatch.

After redispatch, the national configuration has 7.88% higher costs than the nodal model. Note that we assume that all generators can be redispatched in our model, such that redispatch costs in reality might be higher. Also, in our zonal market clearing problem, we do not consider critical elements within zones and assume that the demand is inelastic and must be fully satisfied in any feasible allocation. In comparison, the average daily redispatch costs in Germany between 2020 and 2022 amount to roughly kEUR 7,200 (Bundesnetzagentur, 2022).<sup>17</sup> The average daily redispatch costs in Germany in 2022 were even at around kEUR 11,600, having increased by almost 100% compared to 2021. We assume zero redispatch for a nodal system that satisfies  $\Psi^{DC}$ , although in practice a post-processing step is required to ensure that the DCOPF solution is ACOPF-feasible (Taheri & Molzahn, 2024). In the US, this post-processing depends on the ISO and involves using an

<sup>16</sup>The values are obtained by computing  $\frac{x-100}{y} - 100$ , where  $x$  is the zonal cost for a specific configuration and  $y$  is the nodal cost.

<sup>17</sup>These costs include power- and voltage-related redispatch measures, countertrading activities and redispatch test procedures.

ACOPF model to adjust the DCOPF solution, accounting for real power losses, voltage magnitudes, and reactive power needs (California ISO, 2024).

### 3.1.1. Welfare losses with Euphemia - Impact of Non-Uniform Pricing

Euphemia maximizes welfare subject to linear and uniform prices, which is different from unconstrained welfare maximization. In our analysis, the average daily welfare loss associated with Euphemia compared to the national configuration (without any network constraints) is 0.34% – or EUR 109,801.24 in absolute terms. This is comparable with previous estimate of 0.05% as a relative loss (Meeus et al., 2009).<sup>18</sup> Disregarding market coupling, the cuts introduced by the Euphemia algorithm to get to linear prices do not deteriorate the outcome by a lot. After redispatch, Euphemia suffers an average daily loss of 7.9% (or kEUR 2,859.80) in total costs compared to the nodal allocation rule. We argue that the national, zonal, or Euphemia models differ only marginally in terms of allocation, and only a transition to a nodal allocation rule would substantially affect the average generation and redispatch costs.

### 3.2. Price Levels

Table 4 provides average prices over all hours of the weeks under consideration, while Table 5 illustrates median prices and Table 6 price standard deviations for all computed prices under the respective allocation and pricing rule.

in EUR/MWh	National	2 Zones (k)	2 Zones (s)	3 Zones	4 Zones	Nodal
IP	45.92	45.45	46.56	44.90	44.37	46.63
CH	40.13	40.53	40.81	40.21	41.35	44.79
Join	46.31	48.04	46.0	45.51	48.41	47.65
Euphemia	47.08					

Table 4: Average Prices

in EUR/MWh	National	2 Zones (k)	2 Zones (s)	3 Zones	4 Zones	Nodal
IP	48.66	48.44	48.84	48.23	45.79	48.66
CH	31.09	31.17	31.27	31.11	38.53	49.41
Join	48.68	49.37	48.60	48.31	49.27	49.19
Euphemia	48.84					

Table 5: Median Prices

Note that the mean BZR price for the weeks under consideration was EUR/MWh 40.17 and the standard deviation EUR/MWh 18.51, computed bi-hourly based on a linear relaxation.

Average CH (Convex Hull) prices are slightly lower compared to the other pricing rules under consideration, with lower standard deviation and irrespective of the allocation rule. In contrast,

<sup>18</sup>Note that the 0.05% relative welfare loss does not correspond to the official Euphemia implementation, but to a simulation that considers block order restrictions (Meeus et al., 2009).

in EUR/MWh	National	2 Zones (k)	2 Zones (s)	3 Zones	4 Zones	Nodal
IP	19.76	19.55	19.79	19.45	19.57	19.54
CH	14.43	14.42	14.74	14.39	14.32	16.78
Join	19.97	20.45	20.12	20.34	20.64	20.06
Euphemia	20.61					

Table 6: Price Standard Deviation

median prices are at comparable levels across all pricing rules. Since CH prices are unaffected by pre-determined generator commitments, they tend to be lower and more stable. In particular, prices can be set by a cheaper – yet uncommitted – generator (Schiro et al., 2016). In contrast, average Euphemia prices tend to be slightly higher than zonal prices, while median prices are in the same ranges. This finding implies that the price-setting generator is usually identical for Euphemia and zonal prices, yet sometimes the Euphemia algorithm introduces a cut that disallows a generator that would otherwise be dispatched. As a result, a higher-price generator may set the price.

Price distributions are generally similar across the different zonal configurations for a specific pricing rule. Cross-zonal flow constraints are rarely tight and thus zonal prices are identical to national (single-zone) prices in many hours. This observation suggests that splits into only a few zones, on average, have little impact on prices and thus provide few locational incentives. Table 7 illustrates that, on average, no major price discrepancies between zones can be expected. The zones are depicted in Figure 1.

in EUR/MWh	National	2 Zones (k)	2 Zones (s)	3 Zones	4 Zones
Zone 1	45.92 (19.76)	46.88 (19.69)	48.36 (19.87)	45.42 (19.68)	42.43 (19.22)
Zone 2		44.02 (19.30)	44.76 (19.55)	44.28 (19.37)	45.58 (19.96)
Zone 3				45.02 (19.28)	44.08 (19.05)
Zone 4					45.38 (19.86)

Table 7: IP Zonal Prices Average and Standard Deviation per Zone

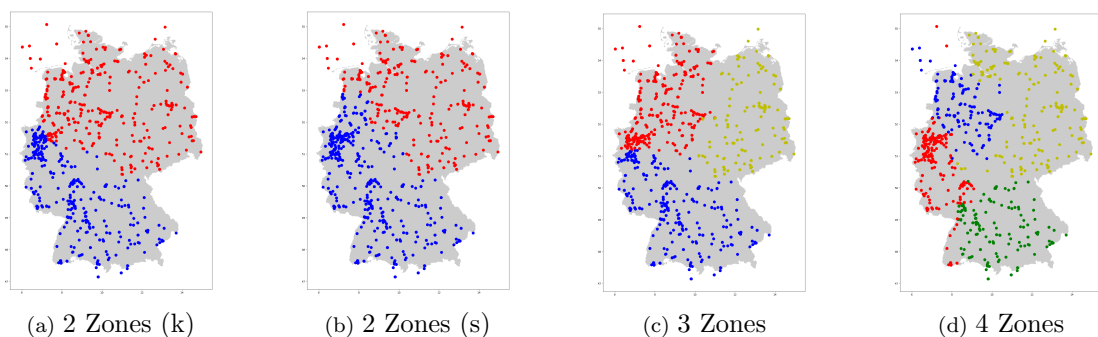


Figure 1: Zonal Configurations

A more in-depth examination of zonal pricing reveals the impact of cross-zonal flows in equalizing prices across different zones. Specifically, while southern zones face a relative shortage of generation capacity compared to demand, the capacity of cross-zonal transmission lines is typically



high enough to transmit electricity from northern zones. Our sensitivity analysis revealed that if cross-zonal flows were limited or prohibited, zonal prices can display differences of more than 30 EUR/MWh between northern and southern regions on some days. The small differences in zonal prices observed in Table 7 are due to the cross-zonal transmission capacity. As described in Section 2.1.2, to compute a zonal solution, we model the interconnectors individually but we do not consider critical network elements and loop flows, which might decrease the available capacity between zones in practice.

Under nodal pricing (ca. 40,000 prices per day for 1670 nodes – compared to, e.g., 24 national prices per day) more price outliers were observed than under zonal pricing. For instance, 0.13% of IP (Integer Programming) prices had to be capped 100 EUR/MWh under the zonal configurations, compared to 0.25% under nodal pricing. Without capping, the maximum observed IP and Join price would be as high as 62,000 EUR/MWh for an hour of extreme scarcity. Note that SDAC also imposes a price cap of 5,000 EUR/MWh for such periods. CH prices, in contrast, are less prone to outliers, peaking at 423 EUR/MWh. Thus tight flow constraints can increase price levels in the short run. The zonal allocation rules oversimplify the transmission network to an extent that nodal prices can hardly be lower, even without congestion. In contrast, when congestion is present in parts of the grid, nodal prices will be higher, resulting in higher average and median prices. Upon further analysis, it was found that nodal prices have high sensitivity to transmission line susceptances, a phenomenon previously described in Bichler & Knörr (2023).

Figure 2 illustrates nodal IP, CH, and Join prices, averaged over all hours and sorted in ascending order. The dashed horizontal and vertical lines mark the 5th and 95th percentiles for prices and nodes, respectively. Additionally, the figure shows the average national prices and the national average including a uniform EUR/MWh price adder for redispatch costs. This price adder is calculated as the total redispatch costs (ca. EUR 478 million) divided by the total demand (ca. 83.3 TWh), and equals 5.73 EUR/MWh. Notably, with redispatch taken into account, higher average prices are expected at some of the nodes. For the majority of nodes, however, the change in average prices is minor or even negative under nodal pricing.

Figure 3 maps these average prices to their geographical locations. As much of the electricity supply, particularly wind energy, is located in Northern Germany, we observe that average nodal prices tend to be higher in Southern Germany. Generally, this price gap is moderate and provides locational incentives for market participants. The choice of pricing rule does not seem to have a major effect on average price levels.

We observe the highest prices in Northern Central Germany in a region with a high share of expensive biomass energy and the lowest prices in the Alps region with inexpensive hydro energy. The associated nodes are relatively isolated with frequent congestion. This behavior might follow from imprecise estimations of generation costs and line limits described in Section 2.2, yet price outliers can also be observed in the ENTSO-E report (ENTSO-E, 2022).

Nodal prices typically vary across locations for each hour, and thereby set locational incentives for flexible units or storage. As seen in Figure 4, standard deviations of nodal prices resemble

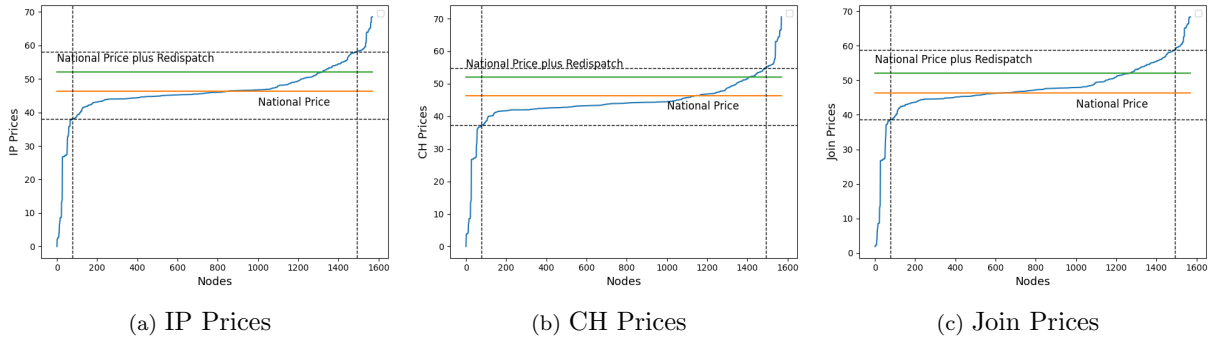


Figure 2: Sorted Nodal Prices [EUR/MWh]

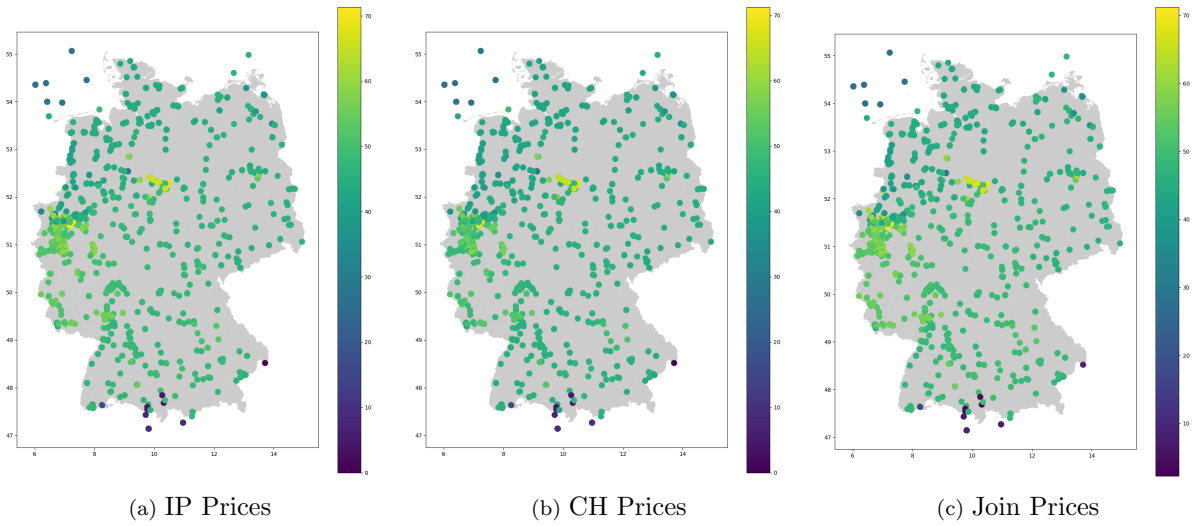


Figure 3: Average Nodal Prices [EUR/MWh]

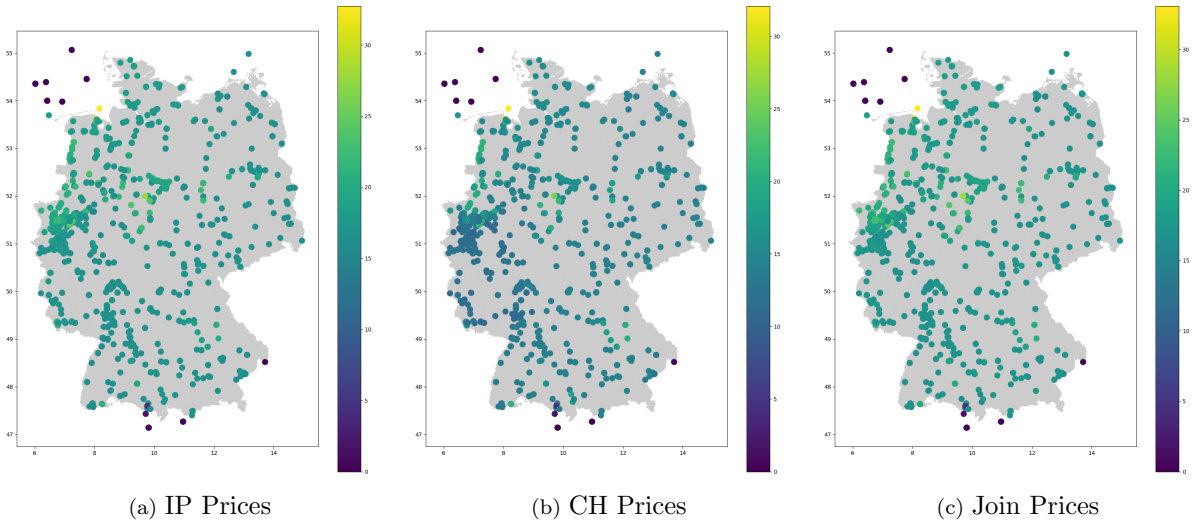


Figure 4: Standard Deviation Nodal Prices [EUR/MWh]

each other across nodes and pricing rules. Figure 5 illustrates the distribution of hourly standard deviations of prices across nodes, with mean and median standard deviations as solid and dashed lines, respectively. The nodal price variances can be substantial. For example, in the extreme first hour of 2009/11/23, IP prices vary across the country between 0 EUR/MWh and 100 EUR/MWh. This sets incentives for demand response and short-term adjustments in particular in energy-intensive industrial production. Persistent high nodal prices signal transmission bottlenecks and direct investments in grid expansion.

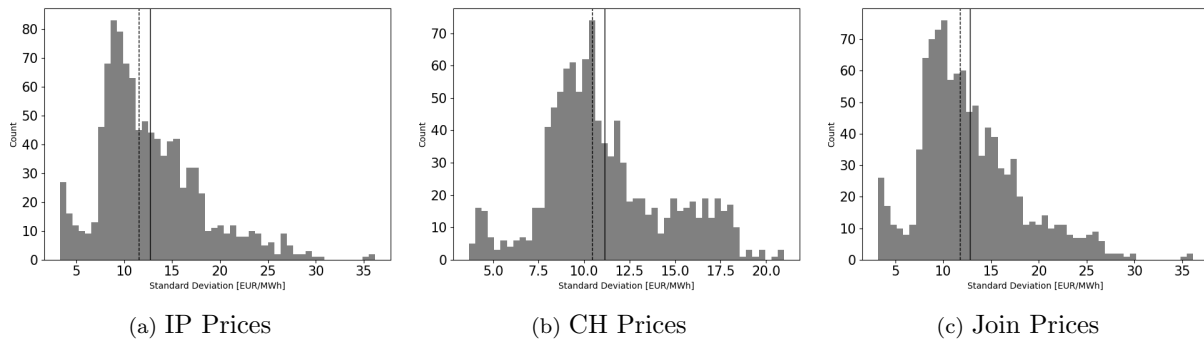


Figure 5: Histograms of Hourly Standard Deviations Across Nodes [EUR/MWh]

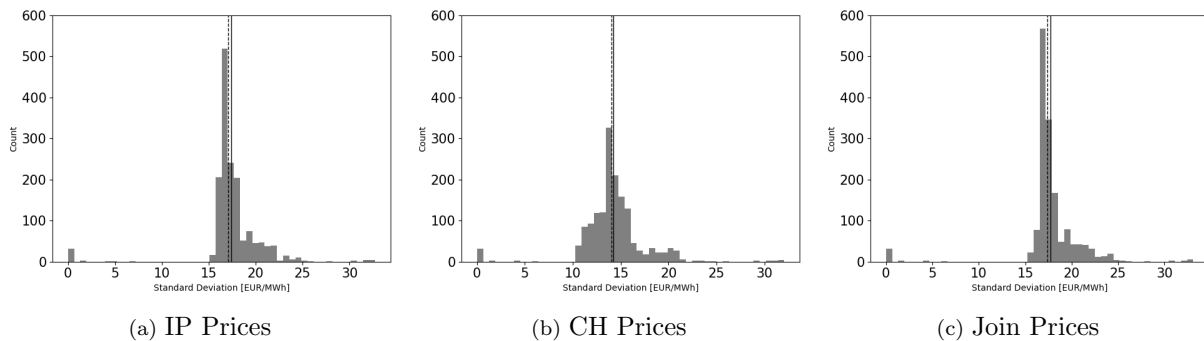


Figure 6: Histograms of Nodal Standard Deviations Across Hours [EUR/MWh]

A primary goal in the design of new bidding zones is the reduction of price variance within a zone (ACER, 2022b), which signals congestion. Tables 6 and 7 indicate that the standard deviation of zonal prices does not decrease with the number of zones. However, varying prices can have two main reasons: congestion and temporal changes in supply and demand. Figure 5 considers hourly standard deviations of prices across all nodes, meaning it illustrates the price variance based on grid congestions in each hour, which we refer to as *congestion-based standard deviation*. In contrast, Figure 6 includes histograms of the standard deviation of nodal prices across all hours, meaning it illustrates the price variance based on temporal effects of supply and demand at each node, which we refer to as *time-based standard deviation*. Together, Figures 5 and 6 represent a composition of the standard deviations reported for nodal prices in Table 6. Note that prices at a single node can vary substantially over time due to changes in supply and demand. This time-based standard deviation exceeds the congestion-based standard deviation. For example, IP prices exhibit a mean congestion-

based standard deviation of EUR/MWh 12.68, compared to a mean time-based standard deviation of EUR/MWh 17.39. These numbers provide evidence that temporal fluctuations of supply and demand have greater impact on price variance compared to congestion.

Tables 8 and 9 provide a more detailed variance decomposition for IP prices under all zonal configurations. In particular, Table 8 indicates the congestion-based standard deviation of nodal IP prices, averaged over all nodes assigned to a zone. Equivalently, Table 9 summarizes the time-based standard deviations grouped by zone. Specifically, the time-based standard deviation always exceeds the congestion-based standard deviation, implying that temporal effects drive price variance more than congestion effects. At the same time, the time-based standard deviation varies only little across allocation rules, suggesting that nation-wide fluctuations in supply and demand, on average, affect all price zones equally. In contrast, the congestion-based standard deviation has a slightly decreasing trend with more zones, indicating that zonal splits can reduce price variance at least for some of the zones (e.g., Zone 3). This effect, however, is not consistent across all zones, implying that the cross-zonal lines fail to encompass all congested lines. Consequently, the computed dispatch does not account for the remaining intra-zonal congestion, necessitating costly redispatch under all zonal models, as shown in Table 2. Dobos et al. (2025) demonstrate that the proposed zone configurations lack stability and fail to effectively segregate nodes along congested lines. As a result, the congestion-based standard deviation exhibits minimal reduction as the number of zones increases, and redispatch costs remain high.

Before moving to the next section, let us emphasize that day-ahead prices alone cannot fully determine the desirability of different market designs or bidding zone configurations. These prices do not reflect: (1) the magnitude of redispatch costs, (2) network tariffs (*Netzentgelte*), which TSOs use to cover redispatch costs and maintain network infrastructure, (3) congestion revenues received by TSOs, and (4) payments required to address non-convexities in generation profiles (see Section 2.1.3).

in EUR/MWh	National	2 Zones (k)	2 Zones (s)	3 Zones	4 Zones
Zone 1	12.19	12.77	12.71	11.99	12.25
Zone 2		10.25	10.26	12.32	11.16
Zone 3				6.27	6.07
Zone 4					13.21

Table 8: Average Congestion-Based Standard Deviation of Nodal IP Prices

in EUR/MWh	National	2 Zones (k)	2 Zones (s)	3 Zones	4 Zones
Zone 1	17.39	17.09	17.39	16.58	18.28
Zone 2		17.65	17.40	18.21	17.56
Zone 3				17.00	17.20
Zone 4					16.12

Table 9: Average Time-Based Standard Deviation of Nodal IP Prices

### 3.3. GLOCs, LLOCs, MWPs

The average daily GLOCs, LLOCs, and MWPs are summarized in Tables 10–12, respectively. Recall from Section 2.1.3 that GLOCs represent the opportunity costs incurred if agents are allowed to deviate from the current allocation to achieve their individual maximum profit, given the market-clearing prices. LLOCs are a subclass of GLOCs quantifying the opportunity costs obtained when agents are not allowed to change their commitment status. MWPs are the minimum compensation provided to market agents, ensuring they do not incur losses (i.e., negative utility) given the market-clearing prices. GLOCs and LLOCs are not paid in practice. MWPs, however, are paid in US electricity markets and are generally not covered directly by revenues obtained from the buyers through energy purchases in the day-ahead market.

in EUR	National	2 Zones (k)	2 Zones (s)	3 Zones	4 Zones	Nodal
IP	2,975,070.52	2,666,810.11	3,332,450.37	2,563,874.88	3,130,778.9	5,469,460.3
CH	124,235.5	162,896.45	520,529.19	141,048.26	717,983.02	382,104.15
Join	981,496.35	1,880,938.84	1,001,437.75	1,801,132.46	2,616,044.17	4,792,706.62
Euphemia	1,002,357.56					

Table 10: Average Daily GLOCs

in EUR	National	2 Zones (k)	2 Zones (s)	3 Zones	4 Zones	Nodal
IP	0.00	0.00	0.00	0.00	0.00	0.00
CH	11,388.11	31,280.46	109,165.0	22,230.84	174,685.4	184,626.79
Join	883.43	3,539.37	1,432.85	1,473.60	15,489.43	36,927.06
Euphemia	0.00					

Table 11: Average Daily LLOCs

in EUR	National	2 Zones (k)	2 Zones (s)	3 Zones	4 Zones	Nodal
IP	32,400.08	45,448.71	30,881.3	21,122.54	42,156.28	202,106.42
CH	8,691.04	38,029.2	78,808.99	19,794.25	161,948.7	114,669.73
Join	1,153.58	7,375.58	1,780.6	797.12	1,364.48	22,105.27
Euphemia	0.00					

Table 12: Average Daily MWPs

By definition, CH prices minimize GLOCs, and on average, they are substantially lower compared to both IP and Join prices, irrespective of the chosen allocation rule. Similar orders of magnitude for GLOCs are observed across all zonal allocation rules, including Euphemia. In contrast, nodal pricing results in the highest GLOCs, aligning with the higher average prices presented in Table 4. Higher prices imply greater forgone profits for generators and increase GLOCs. Generators in nodal markets face stronger incentives to deviate from the optimal outcome, necessitating penalties – a common practice in many U.S. markets (Bichler et al., 2022).

As a natural subset of GLOCs, LLOCs follow a similar pattern, with the highest values occurring under nodal pricing, once again correlated with higher average prices. IP pricing ensures zero

LLOCs, as discussed in Section 2.1.3, ensuring reliable congestion signals, meaning that price differences between adjacent nodes arise only if the line connecting them is congested. In this case, the price difference precisely reflects the marginal value of transmission capacity. In contrast, CH pricing consistently results in the highest LLOCs, supporting observations that congestion signals may be flawed (Schiro et al., 2016). This is especially relevant under a nodal allocation rule considering all transmission lines. The Join pricing rule yields substantially fewer LLOCs than CH pricing, indicating a superior quality of congestion signals.

In terms of average MWPs to compensate generator losses, only the Euphemia algorithm generates zero MWPs, albeit at the expense of welfare losses. An interesting observation is that the welfare losses of Euphemia – as discussed in Section 3.1 – exceed, on average, the MWPs required under a national welfare-maximizing allocation (i.e., a zonal model as described in Section 2.1.2 with a single zone), irrespective of the pricing rule. This implies that the additional generated welfare could potentially cover the MWPs under a national allocation, resulting in a net welfare gain. Under nodal pricing, MWPs tend to increase compared to zonal pricing, particularly for IP pricing. This can be attributed to the fact that under a national allocation rule, there exists a single hourly IP price set at the variable cost of the marginal generator. With positive fixed costs and constant variable costs, such a generator will inevitably incur a loss and necessitate MWPs under IP pricing. In contrast, nodal pricing involves several hourly IP prices and price-setting generators across the network, leading to higher overall MWPs. Conversely, the Join pricing rule generates lower MWPs than IP and CH pricing, constituting a negligible share of the total costs outlined in Table 2.

In summary, GLOCs, LLOCs, and MWPs follow similar patterns across different zonal configurations, but increase with nodal pricing. Concerning pricing rules, IP, CH, and Euphemia each minimize a specific class of lost opportunity costs. However, the Join pricing rule stands out by striking a remarkable balance between low MWPs and LLOCs. At the expense of slightly increased GLOCs, Join prices facilitate marginal side-payments and maintain a high quality of congestion signals.

### *3.4. Analysis of Representative Days*

To corroborate our findings, we examine three selected days in greater detail. Specifically, we analyze November 23 for its low price levels, March 10 for medium price levels, and February 18 for high price levels.

The generation costs for each of these days are presented in Table 13. On 2009/11/23, characterized by warm and windy conditions with low demand, generation costs were minimal, and no congestion occurred in the zonal models, resulting in identical allocations for the national, 2 Zones (k) and 3 Zones configurations. In contrast, February 18, as a cold and cloudy day, saw substantially higher generation costs, but cross-zonal flow constraints had little impact on the allocation. Across all days, the shift from zonal to nodal pricing led to a similar increase in generation costs.

Table 14 indicates that minimum cost redispatch costs are not correlated with the generation costs presented in Table 13. This observation underscores that zonal models lack a representation

of transmission bottlenecks, necessitating redispatch regardless of the zonal configuration or day.

in kEUR	National	2 Zones (k)	2 Zones (s)	3 Zones	4 Zones	Nodal
2009/11/23	26,673.74	26,673.74	27,088.39	26,673.74	26,818.18	29,596.10
2009/03/10	31,401.65	31,494.31	31,494.38	31,661.73	31,647.02	35,200.69
2009/02/18	46,287.23	46,471.33	46,287.57	46,287.34	46,432.68	49,303.25

Table 13: Generation Costs: Nov 23, Mar 10, Feb 18

in kEUR	National	2 Zones (k)	2 Zones (s)	3 Zones	4 Zones	Nodal
2009/11/23	5,004.46	4,998.43	3,921.76	5,009.53	5,034.83	0
2009/03/10	6,295.55	6,302.74	6,302.72	6,135.43	6,136.75	0
2009/02/18	3,603.04	3,419.32	3,602.7	3,602.93	3,457.77	0

Table 14: RD-Min-Cost Redispatch Costs: Nov 23, Mar 10, Feb 18

In summary, as outlined in Table 15, the nodal allocation rule consistently yields lower total costs than any zonal configurations. Despite modest cost savings, nodal allocation enables locational price signals and incentivizes a long-run equilibrium.

On 2009/11/23 and 2009/03/10, the allocation obtained from the Euphemia algorithm is identical to the national configuration, and no welfare loss occurs. On 2009/02/18, costs under the Euphemia algorithm are slightly higher by 0.36%. This validates our assertion that differences between zonal models – including Euphemia – are minor and nuanced, while nodal pricing constitutes a more substantial change in generation and redispatch costs.

in kEUR	National	2 Zones (k)	2 Zones (s)	3 Zones	4 Zones	Nodal
2009/11/23	31,678.20	31,672.17	31,010.15	31,683.27	31,853.01	29,596.10
2009/03/10	37,697.20	37,797.05	37,797.10	37,797.16	37,783.77	35,200.69
2009/02/18	49,890.27	49,890.65	49,890.27	49,890.27	49,890.45	49,303.25

Table 15: Total Costs: Nov 25, Mar 10, Feb 18

Figure 7 illustrates the locational IP, CH, and Join prices for the three selected days, averaged over 24 hours. As previously discussed, the prices on these days exhibit a positive correlation with generation costs, with the exception of Northern Central and Southern Germany with consistent price outliers due to local supply structures. Notably, even though at lower price levels, a more distinct north-south price gradient can be observed on 2009/11/23 compared to 2009/03/10. Specifically, on 2009/11/23, demand is low nationwide, yet inexpensive electricity from the north cannot be transmitted to the south, leading to uneven price levels. In contrast, on 2009/03/10, with higher demand but a balanced grid, prices are uniform across the country. This phenomenon holds for all three pricing rules. The simplified zonal models fail to detect any transmission bottlenecks on 2009/11/23, i.e., cross-zonal constraints are not tight and there are no price variations between zones. Consequently, if the zone configurations are suboptimal, zonal prices do not signal scarcity appropriately.

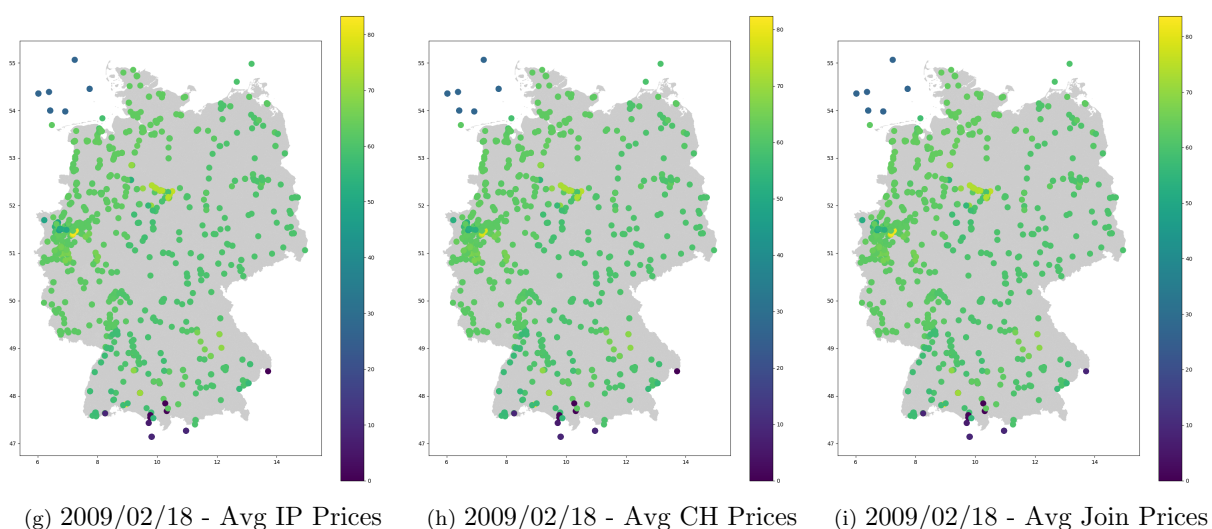
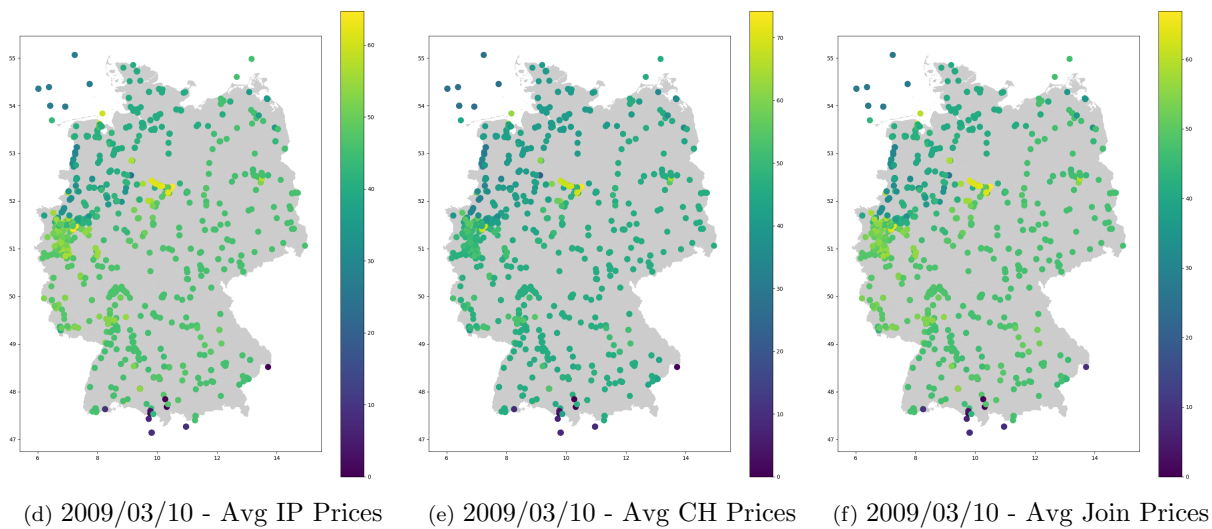
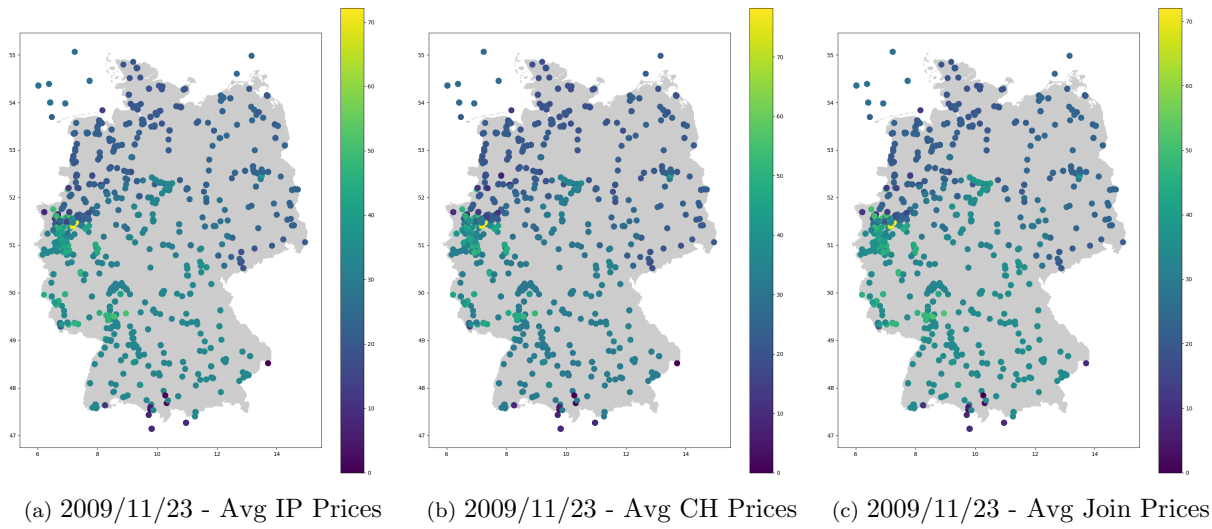


Figure 7: Average Nodal Prices



Table 16 summarizes the GLOCs, LLOCs, and MWPs for each selected day. On the low-demand day of 2009/11/23, a Walrasian equilibrium as in Definition 1 is attainable for the national, 2 Zones (k) and 3 Zones models, resulting in zero GLOCs, LLOC, and MWPs. Crucially, all three pricing rules successfully obtain these equilibrium prices. The Walrasian equilibrium, however, can only persist before redispatch is considered and ceases to exist when nodal transmission constraints are taken into account.

GLOCs, LLOCs, and MWPs do not necessarily increase with average price levels. For nodal pricing, they remain relatively consistent across all days. There is a substantial increase for zonal pricing on the medium-price day of 2009/03/10, compared to the high-price day of 2009/02/18. This indicates that incentives to deviate hinge more on the quality of the price signal than the actual price level.

The simplification inherent in zonal models, which leads to redispatch, does not necessarily imply better economic properties of prices. For example, on 2009/02/18, zonal IP and Join prices result in higher GLOCs than nodal pricing. Specifically, a few zonal prices are insufficient to incentivize many market participants to adhere to the allocation.

As discussed above, CH prices always minimize GLOCs, and IP prices always yield zero LLOCs. Although GLOCs are reduced by CH pricing compared to both IP and Join pricing, their LLOCs, and often MWPs, experience a slight increase. In practical terms, this implies that congestion signals are more distorted and higher side-payments are required. In contrast, the Join pricing rule achieves a favorable trade-off between LLOCs and MWPs, requiring only slightly higher penalties (corresponding to GLOCs) than IP pricing.

### *3.5. Discussion*

Our numerical experiments with the BZR data set provide insights into different market clearing models, pricing rules, and their short-term economic implications on day-ahead markets. Nodal pricing tends to result in slightly higher average prices compared to zonal pricing, irrespective of the chosen zonal configuration. However, transmission constraints can be violated and necessitate costly redispatch measures. As a result, a zonal pricing selects an inefficient dispatch, and even if redispatch is conducted at minimal costs, the total system costs will be significantly higher than under nodal pricing. Given the steep increase of redispatch costs in recent years, this effect is likely to magnify in the future.

Interestingly, the choice of zonal configuration did not substantially impact prices. All zonal configurations suggested by ACER in the BZR simplify the network to an extent that opting for two, three, or four zones yields similar results regarding the average prices and the price standard deviation. Analyses of individual days show that congestion arises, but not necessarily at the cross-zonal lines but within zones. While nodal prices may vary between nodes, these differences incentivize short-term demand response on nodes where this is most helpful for overall system stability. If such price differences persist over more extended time periods, they also set investment incentives for generators and grid expansion. Note that our analysis does not take such incentives

in kEUR		IP	CH	Join	in kEUR		IP	CH	Join
National	GLOC	0	0	0	National	GLOC	2,274.12	52.96	924.26
	LLOC	0	0	0		LLOC	0	16.61	1.93
	MWP	0	0	0		MWP	134.79	13.33	0
2 Zones (k)	GLOC	0	0	0	2 Zones (k)	GLOC	3,539.04	45.62	3,539.04
	LLOC	0	0	0		LLOC	0	8.64	0
	MWP	0	0	0		MWP	164.79	4.60	164.79
2 Zones (s)	GLOC	1,774.99	1,167.39	1,774.99	2 Zones (s)	GLOC	4,730.19	260.35	918.13
	LLOC	0	515.51	0		LLOC	0	27.39	0.98
	MWP	0	117.40	0		MWP	84.07	26.24	1.01
3 Zones	GLOC	0	0	0	3 Zones	GLOC	3,872.84	213.04	3,872.84
	LLOC	0	0	0		LLOC	0	172.13	0
	MWP	0	0	0		MWP	0	153.07	0
4 Zones	GLOC	1,824.29	791.11	1,824.29	4 Zones	GLOC	787.65	751.28	970.31
	LLOC	0	292.25	0		LLOC	0	101.38	5.95
	MWP	0	118.68	0		MWP	109.6	132.42	3.26
Nodal	GLOC	1,290.22	273.99	1,507.04	Nodal	GLOC	1,906.47	256.65	1,942.01
	LLOC	0	149.17	27.31		LLOC	0	158.07	34.79
	MWP	167.98	96.80	34.41		MWP	191.19	84.14	20.73

(a) GLOC, LLOC, MWP for 2009/11/23

(b) GLOC, LLOC, MWP for 2009/03/10

in kEUR		IP	CH	Join
National	GLOC	4,442.86	318.73	2,618.64
	LLOC	0	29.04	9.31
	MWP	41.66	27.1	8.59
2 Zones (k)	GLOC	2,258.24	502.83	2,600.59
	LLOC	0	166.68	6.14
	MWP	35.23	155.67	6.02
2 Zones (s)	GLOC	1,727.29	319.07	1,956.49
	LLOC	0	16.06	8.01
	MWP	26.55	23.60	13.90
3 Zones	GLOC	3,284.92	318.84	3,284.92
	LLOC	0	28.68	0
	MWP	46.26	26.01	46.26
4 Zones	GLOC	1,523.92	464.18	2,642.54
	LLOC	0	136.24	6.03
	MWP	35.19	102.14	5.92
Nodal	GLOC	551.27	241.74	624.76
	LLOC	0	51.26	25.56
	MWP	73.43	27.55	20.02

(c) GLOC, LLOC, MWP for 2009/02/18

Table 16: Daily GLOCs, LLOCs, MWPs

into account and assumes static demand. Nevertheless, long-run effects related to inefficient placement and technology choice for production, consumption and grid expansion are important factors to consider when evaluating a market clearing model.

Given the absence of Walrasian equilibria, any pricing rule – regardless of zonal or nodal pricing – must balance economic properties such as welfare gains and the participants’ lost opportunity costs. The currently used Euphemia algorithm leads to welfare losses and is computationally expensive. It avoids paradoxically accepted bids but may result in paradoxically rejected bids. Our experiments show that the welfare losses of Euphemia exceed the alternative costs of make-whole payments. Moreover, non-uniform pricing rules, such as CH pricing, achieve low make-whole payments for paradoxically accepted bids while maintaining the optimal allocation and scaling in polynomial time. The findings provide support for non-uniform pricing as it is currently being discussed in the context of the Capacity Allocation and Congestion Management (CACM) Regulations (All NEMO Committee, 2023). CH pricing minimizes GLOCs, but our results confirm previous findings that high MWPs are necessary. IP pricing, the prevailing rule in U.S. markets, ensures effective congestion signals but requires very high MWPs. The Join pricing rule strikes a balance between LLOCs and MWPs, ensuring low side-payments and good congestion signals.

#### 4. Conclusion

The discussion surrounding zonal and nodal pricing has a long history. The European electricity market has employed zonal pricing for many years, often with large, nationwide price zones. However, the ongoing energy transition requires a reevaluation of price zones. Based on recent data released by ENTSO-E in the context of the EU Bidding Zone Review process, we compare the short-run effects of various zonal and nodal pricing rules for the German power market. Our findings indicate that, in terms of system costs and price signals, a nodal allocation rule with non-uniform pricing leads to the lowest total costs. Costly redispatch is mitigated, and the average prices increase only slightly. Additionally, pricing rules such as Join pricing require very low side-payments, while efficiently signaling transmission bottlenecks. In contrast, the proposed zonal configurations only differ marginally regarding system costs and the differences in average prices across zones are low. Also, the effect of zonal splits on price standard deviations is low, and we do not find evidence for significant reductions in redispatch costs resulting from such splits. The study does not say that there cannot be congestion on cross-zonal lines leading to significant price differences between zones at certain times. However, in the BZR dataset that was intended to inform ACER based on realistic demand and supply scenarios (the 2009 climate year), we do not find significant price differences. Fears of substantial price differences after a zonal split might be overrated based on this comprehensive and up-to-date dataset. Importantly, we could provide a fair comparison with nodal pricing rules and show that the welfare gains are around 7-8%, depending on the zonal configuration.

## References

- ACER (2022a). *Decision no 11/2022 of the european union agency for the cooperation of energy regulators*. <https://www.acer.europa.eu/sites/default/files/documents/Individual%20Decisions/ACER%20Decision%2011-2022%20on%20alternative%20BZ%20configurations.pdf>
- ACER (2022b). *List of alternative bidding zone configurations to be considered for the bidding zone review*.
- Ahunbay, M. c., Bichler, M., & Knörr, J. (2024). Pricing optimal outcomes in coupled and non-convex markets: Theory and applications to electricity markets. *Operations Research*. <https://doi.org/10.1287/opre.2023.0401>
- All NEMO Committee (2022). *CACM annual report 2021*. [https://www.nemo-committee.eu/assets/files/nemo\\_CACM\\_Annual\\_Report\\_2021\\_220630-4e7321983974b812f28730a301c9f7d9.pdf](https://www.nemo-committee.eu/assets/files/nemo_CACM_Annual_Report_2021_220630-4e7321983974b812f28730a301c9f7d9.pdf)
- All NEMO Committee (2023). *Non-uniform pricing: Explanatory note*. <https://www.nemo-committee.eu/assets/files/sdac-non-uniform-pricing-explanatory-note.pdf>
- Ambrosius, M., Egerer, J., Grimm, V., & van der Weijde, A. H. (2022). Risk aversion in multilevel electricity market models with different congestion pricing regimes. *Energy Economics*, 105, 105701.
- Ambrosius, M., Grimm, V., Kleinert, T., Liers, F., Schmidt, M., & Zöttl, G. (2020). Endogenous price zones and investment incentives in electricity markets: An application of multilevel optimization with graph partitioning. *Energy Economics*, 92, 104879.
- Aravena, I., Leté, Q., Papavasiliou, A., & Smeers, Y. (2021). Transmission capacity allocation in zonal electricity markets. *Operations Research*, 69, 1240–1255. <https://doi.org/10.1287/opre.2020.2082>
- Aravena, I. & Papavasiliou, A. (2016). Renewable energy integration in zonal markets. *IEEE Transactions on Power Systems*, 32, 1–1. <https://doi.org/10.1109/TPWRS.2016.2585222>
- Arrow, K. J. & Debreu, G. (1954). Existence of an equilibrium for a competitive economy. *Econometrica: Journal of the Econometric Society*, 265–290.
- Baldwin, E. & Klemperer, P. (2019). Understanding preferences: demand types, and the existence of equilibrium with indivisibilities. *Econometrica*, 87(3), 867–932.
- Bertsch, J., Hagspiel, S., & Just, L. (2016). Congestion management in power systems. *Journal of Regulatory Economics*, 50(3), 290–327.
- Bichler, M., Knoerr, J., & Maldonado, F. (2022). Pricing in non-convex markets: How to price electricity in the presence of demand response. *Information Systems Research*, 1(to appear).
- Bichler, M. & Knörr, J. (2023). Getting prices right on electricity spot markets: On the economic impact of advanced power flow models. *Energy Economics*, 126, 106968.
- Bikhchandani, S. & Mamer, J. W. (1997). Competitive equilibrium in an exchange economy with indivisibilities. *Journal of Economic Theory*, 74(2), 385–413.

- Bikhchandani, S. & Ostroy, J. M. (2002). The package assignment model. *Journal of Economic Theory*, 107(2), 377–406.
- Breuer, C., Seeger, N., & Moser, A. (2013). Determination of alternative bidding areas based on a full nodal pricing approach. 1–5. <https://doi.org/10.1109/PESMG.2013.6672466>
- Bundesnetzagentur (2022). *Zahlen zu netzengpassmanagementmaßnahmen – gesamtes jahr 2022*. ([https://www.bundesnetzagentur.de/SharedDocs/Downloads/DE/Sachgebiete/Energie/Unternehmen\\_Institutionen/Versorgungssicherheit/Engpassmanagement/Ganzjahreszahlen2022.pdf](https://www.bundesnetzagentur.de/SharedDocs/Downloads/DE/Sachgebiete/Energie/Unternehmen_Institutionen/Versorgungssicherheit/Engpassmanagement/Ganzjahreszahlen2022.pdf))
- Bundesnetzagentur (2024). *Bundesnetzagentur veröffentlicht daten zum strommarkt 2023*. [https://www.bundesnetzagentur.de/SharedDocs/Pressemitteilungen/DE/2024/20240103\\_SMARD.html](https://www.bundesnetzagentur.de/SharedDocs/Pressemitteilungen/DE/2024/20240103_SMARD.html)
- Burstedde, B. (2012). From nodal to zonal pricing: A bottom-up approach to the second-best. *2012 9th International Conference on the European Energy Market*, 1–8. <https://doi.org/10.1109/EEM.2012.6254665>
- California ISO (2024). *Day-Ahead Market. Operating Procedure*. <https://www.caiso.com/documents/1210.pdf>
- Christie, R., Wollenberg, B., & Wangensteen, I. (2000). Transmission management in the deregulated environment. *Proceedings of the IEEE*, 88(2), 170–195. <https://doi.org/10.1109/5.823997>
- Dobos, T., Bichler, M., & Knörr, J. (2025). Challenges in finding stable price zones in european electricity markets: Aiming to square the circle? *Applied Energy*, 382, 125315. <https://doi.org/https://doi.org/10.1016/j.apenergy.2025.125315>
- Eicke, A. & Schittekatte, T. (2022). Fighting the wrong battle? a critical assessment of arguments against nodal electricity prices in the european debate. *Energy Policy*, 170, 113220.
- ENTSO-E (2022). *Report on the locational marginal pricing study of the bidding zone review process*. [https://eepublicdownloads.blob.core.windows.net/public-cdn-container/clean-documents/Publications/Market%20Committee%20publications/ENTSO-E%20LMP%20Report\\_publication.pdf](https://eepublicdownloads.blob.core.windows.net/public-cdn-container/clean-documents/Publications/Market%20Committee%20publications/ENTSO-E%20LMP%20Report_publication.pdf)
- ENTSO-E (2023). *Bidding zone review*. [https://www.entsoe.eu/network\\_codes/bzr/](https://www.entsoe.eu/network_codes/bzr/)
- ENTSO-E (2024). *Bidding zone review consultative group (bzc)*. [https://eepublicdownloads.blob.core.windows.net/public-cdn-container/clean-documents/Network%20codes%20documents/NC%20EB/2024/241105\\_BZR\\_CG\\_ENTSO-E\\_slides.pdf](https://eepublicdownloads.blob.core.windows.net/public-cdn-container/clean-documents/Network%20codes%20documents/NC%20EB/2024/241105_BZR_CG_ENTSO-E_slides.pdf)
- European Commission (2024). *2040 climate target*. [https://climate.ec.europa.eu/eu-action/climate-strategies-targets/2040-climate-target\\_en](https://climate.ec.europa.eu/eu-action/climate-strategies-targets/2040-climate-target_en)
- Federal Ministry of Education and Research (2024). *German energy transition*. [https://www.bmbf.de/bmbf/en/research/energy-and-economy/german-energy-transition/german-energy-transition\\_node.html](https://www.bmbf.de/bmbf/en/research/energy-and-economy/german-energy-transition/german-energy-transition_node.html)
- Felling, T. & Weber, C. (2018). Consistent and robust delimitation of price zones under uncertainty with an application to central western europe. *Energy Economics*, 75, 583–601. <https://doi.org/https://doi.org/10.1016/j.eneco.2018.09.012>

- Grainger, J. J. & Stevenson, W. D. (1994). *Power System Analysis*. Electrical engineering series. McGraw-Hill.
- Green, R. (2007). Nodal pricing of electricity: how much does it cost to get it wrong? *Journal of Regulatory Economics*, 31(2), 125–149. <https://doi.org/10.1007/s11149-006-9019-3>
- Gribik, P. R., Hogan, W. W., Pope, S. L., et al. (2007). Market-clearing electricity prices and energy uplift. *Cambridge, MA*.
- Grimm, V., Kleinert, T., Liers, F., Schmidt, M., & Zöttl, G. (2019). Optimal price zones of electricity markets: a mixed-integer multilevel model and global solution approaches. *Optimization methods and software*, 34(2), 406–436.
- Grimm, V., Martin, A., Schmidt, M., Weibelzahl, M., & Zöttl, G. (2016). Transmission and generation investment in electricity markets: The effects of market splitting and network fee regimes. *European Journal of Operational Research*, 254(2), 493–509.
- Grimm, V., Rückel, B., Sölch, C., & Zöttl, G. (2021). The impact of market design on transmission and generation investment in electricity markets. *Energy Economics*, 93, 104934.
- Grimm, V., Sölch, C., & Zöttl, G. (2022). Emissions reduction in a second-best world: On the long-term effects of overlapping regulations. *Energy Economics*, 109, 105829.
- Hao, J. & Xu, W. (2008). Extended transmission line loadability curve by including voltage stability constrains. *2008 IEEE Canada Electric Power Conference*, 1–5.
- Hinojosa, V. H. (2020). Comparing corrective and preventive security-constrained dcopf problems using linear shift-factors. *Energies*, 13(3). <https://doi.org/10.3390/en13030516>
- Hirth, L. & Schlecht, I. (2020). *Market-based redispatch in zonal electricity markets: The preconditions for and consequence of inc-dec gaming*. <http://hdl.handle.net/10419/222925>
- Hogan, W. W. & Ring, B. J. (2003). On minimum-uplift pricing for electricity markets. *Electricity Policy Group*.
- Holmberg, P. & Tangerås, T. (2023). A survey of capacity mechanisms: Lessons for the swedish electricity market. *The Energy Journal*, 44(6), 275–304. <https://doi.org/10.5547/01956574.44.6.pho1>
- Hörsch, J., Hofmann, F., Schlachtberger, D., & Brown, T. (2018). Pypsa-eur: An open optimisation model of the european transmission system. *Energy strategy reviews*, 22, 207–215.
- Hua, B. & Baldick, R. (2017). A convex primal formulation for convex hull pricing. *IEEE Transactions on Power Systems*, 32(5), 3814–3823.
- IRENA (2022). *Renewable power generation costs in 2021*.
- Kelso, A. S. & Crawford, V. P. (1982). Job matching, coalition formation , and gross substitute. *Econometrica*, 50, 1483–1504.
- Kost, C., Shammugam, S., Fluri, V., Peper, D., Davoodi Memar, A., & Schlegl, T. (2021). *Levelized cost of electricity - renewable energy technologies*.

- Kumar, A., Srivastava, S., & Singh, S. (2004). A zonal congestion management approach using real and reactive power rescheduling. *IEEE Transactions on Power Systems*, 19(1), 554–562. <https://doi.org/10.1109/TPWRS.2003.821448>
- Kunz, F. & Zerrahn, A. (2015). Benefits of coordinating congestion management in electricity transmission networks: Theory and application to germany. *Utilities Policy*, 37, 34–45. <https://doi.org/https://doi.org/10.1016/j.jup.2015.09.009>
- Kłos, M., Wawrzyniak, K., Jakubek, M., & Oryńczak, G. (2014). The scheme of a novel methodology for zonal division based on power transfer distribution factors. *IECON 2014 - 40th Annual Conference of the IEEE Industrial Electronics Society*, 3598–3604. <https://doi.org/10.1109/IECON.2014.7049033>
- Leuthold, F., Weigt, H., & von Hirschhausen, C. (2008). Efficient pricing for european electricity networks – the theory of nodal pricing applied to feeding-in wind in germany. *Utilities Policy*, 16(4), 284–291. <https://doi.org/https://doi.org/10.1016/j.jup.2007.12.003>. European Regulatory Perspectives
- Li, M., Du, Y., Mohammadi, J., Crozier, C., Baker, K., & Kar, S. (2022). Numerical comparisons of linear power flow approximations: Optimality, feasibility, and computation time. *2022 IEEE Power & Energy Society General Meeting (PESGM)*, 1–5.
- Liberopoulos, G. & Andrianesis, P. (2016). Critical review of pricing schemes in markets with non-convex costs. *Operations Research*, 64(1), 17–31.
- Marien, A., Luickx, P., Tirez, A., & Woitrin, D. (2013). Importance of design parameters on flowbased market coupling implementation. *2013 10th International Conference on the European Energy Market (EEM)*, 1–8. <https://doi.org/10.1109/EEM.2013.6607298>
- Meeus, L., Verhaegen, K., & Belmans, R. (2009). Block order restrictions in combinatorial electric energy auctions. *European Journal of Operational Research*, 196(3), 1202–1206.
- MISO (2023). *Schedule 29A: ELMP for energy and operating reserve market: Ex-post pricing formulations*. [https://docs.misoenergy.org/legalcontent/Schedule\\_29-A\\_-\\_ELMP\\_for\\_Energy\\_and\\_Operating\\_Reserve\\_Market.pdf](https://docs.misoenergy.org/legalcontent/Schedule_29-A_-_ELMP_for_Energy_and_Operating_Reserve_Market.pdf)
- Molzahn, D. K. & Hiskens, I. A. (2019). A survey of relaxations and approximations of the power flow equations. *Foundations and Trends® in Electric Energy Systems*, 4(1-2), 1–221.
- Moreira, F. S., Ohishi, T., & Da Silva Filho, J. I. (2006). Influence of the thermal limits of transmission lines in the economic dispatch. *2006 IEEE Power Engineering Society General Meeting*, 6 pp.
- NEMO Committee (2019). *EUPHEMIA public description: Single price coupling algorithm*. <https://www.epexspot.com/document/40503/Euphemia%20Public%20Description>
- NEMO Committee (2024). *EUPHEMIA public description*. <https://www.nemo-committee.eu/assets/files/euphemia-public-description.pdf>
- Neuhoff, K., Barquin, J., Bialek, J. W., Boyd, R., Dent, C. J., Echavarren, F., Grau, T., von Hirschhausen, C., Hobbs, B. F., Kunz, F., Nabe, C., Papaefthymiou, G., Weber, C., & Weigt, H. (2013). Renewable electric energy integration: Quantifying the value of design of markets for international transmission capacity. *Energy Economics*, 40, 760–772.

- Newbery, D. M. (2023). High renewable electricity penetration: Marginal curtailment and market failure under “subsidy-free” entry. *Energy Economics*, 126, 107011. <https://doi.org/https://doi.org/10.1016/j.eneco.2023.107011>
- Newbery, D. M. & Biggar, D. R. (2024). Marginal curtailment of wind and solar pv: Transmission constraints, pricing and access regimes for efficient investment. *Energy Policy*, 191, 114206. <https://doi.org/https://doi.org/10.1016/j.enpol.2024.114206>
- O’Neill, R. P., Sotkiewicz, P. M., Hobbs, B. F., Rothkopf, M. H., & Stewart, W. R. (2005). Efficient market-clearing prices in markets with nonconvexities. *European Journal of Operational Research*, 1(164), 269–285.
- PJM (2018). *FERC Docket EL 18-34-000: Fast start resources*. <https://www.pjm.com/-/media/committees-groups/task-forces/epfstf/20180118/20180118-fast-start-pricing.ashx>
- Pollitt, M. G. (2023). *Locational Marginal Prices (LMPs) for Electricity in Europe? The Untold Story*. <https://www.jbs.cam.ac.uk/wp-content/uploads/2023/12/eprg-wp2318.pdf>
- Schiro, D. A., Zheng, T., Zhao, F., & Litvinov, E. (2016). Convex hull pricing in electricity markets: Formulation, analysis, and implementation challenges. *IEEE Transactions on Power Systems*, 31(5), 4068–4075.
- Schmitt, N. (2023). *Towards a central dispatch model for european electricity markets*.
- Schröder, A., Kunz, F., Meiss, R., Mendelevitich, R., & von Hirschhausen, C. (2013). *Current and prospective costs of electricity generation until 2050*.
- Simshauser, P. (2025). Competition vs. coordination: Optimising wind, solar and batteries in renewable energy zones. *Energy Economics*, 143, 108279. <https://doi.org/https://doi.org/10.1016/j.eneco.2025.108279>
- St. Clair, H. P. (1953). Practical concepts in capability and performance of transmission lines [includes discussion]. *Transactions of the American Institute of Electrical Engineers. Part III: Power Apparatus and Systems*, 72(6), 1152–1157.
- Stoft, S. (1997). Transmission pricing zones: simple or complex? *The Electricity Journal*, 10(1), 24–31. [https://doi.org/https://doi.org/10.1016/S1040-6190\(97\)80294-1](https://doi.org/https://doi.org/10.1016/S1040-6190(97)80294-1)
- Stott, B., Jardim, J., & Alsac, O. (2009). DC power flow revisited. *IEEE Transactions on Power Systems*, 24(3), 1290–1300.
- Taheri, B. & Molzahn, D. K. (2024). Ac power flow feasibility restoration via a state estimation-based post-processing algorithm. *Electric Power Systems Research*, 235, 110642. <https://doi.org/https://doi.org/10.1016/j.epsr.2024.110642>
- The Federal Government (2024). *Ending coal-generated power*. <https://www.bundesregierung.de/breg-en/service/archive/kohleausstiegsgesetz-1717014>
- Thomassen, G., A, F., R, C., D, P. C., & S, V. (2024). Redispatch and congestion management. Scientific analysis or review, Policy assessment, Anticipation and foresight KJ-NA-31-924-EN-N (online), KJ-NB-31-924-EN-N, Luxembourg (Luxembourg). [https://doi.org/10.2760/853898\(online\),10.2760/871](https://doi.org/10.2760/853898(online),10.2760/871)



- Tiedemann, S., Stiewe, C., Kratzke, C., Hirth, L., Jentsch, M., Damm, N., Gerhardt, N., & Pape, C. (2024). Gebotszonenteilung: Auswirkungen auf den marktwert der erneuerbaren energien im jahr.
- Townsend, A., otterud, A., evin, T., Milligan, M., & Bloom, A. (2014). *Evolution of wholesale electricity market design with increasing levels of renewable generation*. <https://doi.org/10.2172/1159375>
- Trepper, K., Bucksteeg, M., & Weber, C. (2015a). Market splitting in germany – new evidence from a three-stage numerical model of europe. *Energy Policy*, 87, 199–215.
- Trepper, K., Bucksteeg, M., & Weber, C. (2015b). Market splitting in germany – new evidence from a three-stage numerical model of europe. *Energy Policy*, 87, 199–215. <https://doi.org/https://doi.org/10.1016/j.enpol.2015.08.016>
- Voswinkel, S., Felten, B., Felling, T., & Weber, C. (2019). Flow-based market coupling: What drives welfare in europe’s electricity market design? HEMF Working Paper 08/2019, Essen. <https://hdl.handle.net/10419/201591>
- Weinhold, R. & Mieth, R. (2024). Uncertainty-aware capacity allocation in flow-based market coupling. *IEEE Transactions on Power Systems*, 39(1), 147–159. <https://doi.org/10.1109/TPWRS.2023.3265320>
- Wyrwoll, L., Kollenda, K., Müller, C., & Schnettler, A. (2018). Impact of flow-based market coupling parameters on european electricity markets. *2018 53rd International Universities Power Engineering Conference (UPEC)*, 1–6. <https://doi.org/10.1109/UPEC.2018.8541904>
- Yang, Z., Zheng, T., Yu, J., & Xie, K. (2019). A unified approach to pricing under nonconvexity. *IEEE Transactions on Power Systems*, 34(5), 3417–3427.

## Appendix A. Nodal Market Clearing Problem

Parameters		
$B, S, N, T$		Sets of buyers, sellers, network nodes, periods
$n^*$		Reference node
$n_i$	$B \cup S \rightarrow N$	Node in which agent $i \in B \cup S$ is located
$g_s$	[EUR/MWh]	Marginal cost of seller $s \in S$
$h_s$	[EUR/MWh]	No-load cost of seller $s \in S$
$\underline{R}_s$		Minimum uptime of seller $s \in S$ (periods)
$\underline{P}_{st}, \overline{P}_{st}$	[MWh]	Minimum and maximum output of seller $s \in S$ in period $t \in T$
$P_{bt}$	[MWh]	Demand of buyer $b \in B$ in period $t \in T$
$\underline{F}_{nm}, \overline{F}_{nm}$	[MWh]	Minimum and maximum flow on the line connecting $n, m \in N$
$B_{nm}$	[pu]	Susceptance of the line connecting $n, m \in N$
Variables		
$x_{b,nt}$	[MW]	Total consumption of buyer $b \in B$ in node $n \in N$ , period $t \in T$
$y_{s,nt} \geq 0$	[MW]	Total production of seller $s \in S$ in node $n \in N$ , period $t \in T$
$u_{st} \in \{0, 1\}$		Commitment of seller $s \in S$ in $t \in T$
$\phi_{st} \geq 0$		Startup indicator of seller $s \in S$ in period $t \in T$
$\theta_{nt}$		Voltage angle for node $n \in N$ and period $t \in T$

Table A.17: Notation

$$\begin{aligned}
& \min_{x,y,u,\theta} \sum_{s \in S} c_s(y_s) \\
\text{subject to } & \sum_{s \in S} y_{s,nt} - \sum_{b \in B} x_{b,nt} = \sum_{m \in N} -B_{nm}(\theta_{nt} - \theta_{mt}) & \forall n \in N, t \in T \\
& \underline{F}_{nm} \leq B_{nm}(\theta_{nt} - \theta_{mt}) \leq \overline{F}_{nm} & \forall n, m \in N, t \in T \\
& \underline{P}_{st}u_{st} \leq y_{s,nt} \leq \overline{P}_{st}u_{st} & \forall s \in S, t \in T \\
& y_{s,nt} = 0 & \forall s \in S, n \in N \setminus \{n_s\}, t \in T \\
& \phi_{st} \geq u_{st} - u_{s(t-1)} & \forall s \in S, t \in T \setminus \{T_0\} \\
& \sum_{i=t-\underline{R}_s+1}^t \phi_{si} \leq u_{st} & \forall s \in S, t \in T \setminus \{T_0\} \\
& c_s(y_s) = \sum_{t \in T} g_s y_{s,nt} + \sum_{t \in T} h_s u_{st} & \forall s \in S \\
& x_{b,n_b t} = P_{bt} & \forall b \in B, t \in T \\
& x_{b,nt} = 0 & \forall b \in B, n \in N \setminus \{n_b\}, t \in T \\
& \theta_{n^*t} = 0 & \forall t \in T
\end{aligned}$$

## Appendix B. Generation Data

In what follows we outline how we derive the costs and capacities for the renewable (RES) and non-renewable (Non-RES) energy sources (Schmitt, 2023). Since the procedures used to establish these costs differ between RES and Non-RES, we discuss them independently.

### Appendix B.1. Renewables

To derive the costs for RES, we consider the operating costs (OPEX), fuel and CO<sub>2</sub> costs from Table B.18, which are based on (Kost et al., 2021):

RES	OPEX var [EUR/kWh]	Fuel [EUR/kWh]	CO <sub>2</sub> [EUR/kWh]	OPEX fix [EUR/kW/year]
Offshore Wind	0.008	0	0	70
Onshore Wind	0.008	0	0	20
Biomass	0.004	0.04286	0.0026812	160
Photovoltaic	0	0	0	13.3
Hydro	0	0	0	36.64

Table B.18: Costs for RES

We assume that RES require high initial investment costs but relatively low fixed costs. This assumption is attributed to the fact that particularly wind and solar power plants do not require ongoing expenses for fuel purchase and transportation, and have minimal maintenance costs due to the absence of moving parts. Therefore, the fixed cost  $h_s$  is set to 0 for any renewable energy source  $s \in S$ . However, the fixed OPEX cannot be disregarded and are instead incorporated into the variable costs  $g_{st}$ .

We derive the full load hours (FLH) from Table B.19 considering the generated power per production type for the year 2009 and the sum of capacities that are included in the BZR dataset.

RES	FLH [h]
Offshore Wind	3,657.517
Onshore Wind	1,864.482
Biomass	5,756.5427
Photovoltaic	986.3497
Hydro	4,262.101782

Table B.19: FLH for RES

Using the FLH of each production type, we determine the variable cost  $c_{st}$  of a renewable unit  $s \in S$  in a period  $t \in T$  as follows:

$$c_{st} = \text{OPEX}_{\text{var}_{f(s)}} + \text{Fuel}_{f(s)} + \text{CO}_2_{f(s)} + \frac{\text{OPEX}_{\text{fix}_{f(s)}}}{\text{FLH}_{f(s)}}$$

Note that we make the simplifying assumption that variable costs are constant for all time periods. Furthermore, while allocating fixed to variable costs, we do not consider the specific fixed

cost of each plant, which would lead to different variable costs for each plant. Instead, as we use the capacity and generated power per plant type, we derive fixed costs for an average plant per plant type. Table B.20 shows the variable costs for the RES considered in this study. Note that in a final step, these values are anonymized for each power plant by drawing the final costs from a normal distribution, where the calculated variable costs serve as the mean and 1% of these variable costs serve as the standard deviation.

RES	Variable Costs [EUR/MWh]
Offshore Wind	27.24
Onshore Wind	18.73
Biomass	77.34
Photovoltaic	13.84
Hydro	8.60

Table B.20: Variable Costs for RES

The capacity of each RES unit is included in the BZR dataset as a static attribute. This static attribute does not adequately reflect the dynamic nature of RES outputs, which are influenced by weather and time of day. To calculate maximum output, we first determine the total capacity for each RES type and derive a score that represents the ratio of aggregated hourly output to total capacity. The maximum output per period for each RES unit is obtained by multiplying their capacity by this score.

### *Appendix B.2. Non-Renewables*

The BZR dataset includes the variable costs for all thermal plant types. However, the fixed costs are not available, so we use the costs from (Kost et al., 2021), which are shown in Table B.21:

Technology	Variable Costs [EUR/MWh]
Hard Coal	22
Lignite	32
CCGT	20

Table B.21: Fixed Costs for Non-RES

Regarding the units that generate electricity from light oil, we refer to an older publication by Schröder et al. (2013), as more recent publications on the cost of electricity do not include power plants that generate electricity from oil. Concerning oil, Schröder et al. (2013) state fixed costs of 6 EUR/kW/year for the year 2010.

Based on these costs for the different technologies, we estimate yearly fixed costs for each generation unit. However, as fixed costs in our market clearing models are incurred during operating hours, these costs must be distributed over those hours. We approximate these costs using the FLH, which relate a power plant’s generated power to its capacity and represent the number of hours a unit operates at full capacity over a year. Kost et al. (2021) specify the FLH for the year 2020 shown in Table B.22.

Technology	FLH [h]	
	Lower Bound	Upper Bound
Hard Coal	2,600	6,200
Lignite	5,300	7,300
Gas Turbine	500	3,000
CCGT	3,000	8,000

Table B.22: FLH for Non-RES

Note that we assume that any power plant that generates electricity from gas and that is not categorized as a CCGT power plant is associated with the gas turbine technology. Furthermore, since neither Kost et al. (2021) nor Schröder et al. (2013) provide information on FLH for oil power plants, we take the estimates from a recent monitoring report of the Federal Network Agency.<sup>19</sup> In particular, we consider the installed generation capacity of 4.8 GW in 2020 and the net power generation of 4.3 TWh in 2020 implying a value of 895.83 FLH for an average power plant that produces energy from light oil. Therefore, we consider the values depicted in Table B.23 for each of the plant types.

Fuel/Plant Type	OPEX fix [EUR/kW/year]	FLH Lower Bound [h]	FLH Upper Bound [h]
Hard Coal/old 1	22	2600	6200
Hard Coal/old 2	22	2600	6200
Hard Coal/new	22	2600	6200
Lignite/old 1	32	5300	7300
Lignite/old 2	32	5300	7300
Lignite/new	32	5300	7300
Gas/Conventional old 1	20	500	3000
Gas/Conventional old 2	20	500	3000
Gas/CCGT old 1	20	3000	8000
Gas/CCGT old 2	20	3000	8000
Gas/CCGT new	20	3000	8000
Gas/OCGT old	20	500	3000
Gas/OCGT new	20	500	3000
Gas/CCGT present 1	20	3000	8000
Gas/CCGT present 2	20	3000	8000
Light oil/-	6	895.83	895.83

Table B.23: FLH for Non-RES

As the FLH represent a lower bound for the actual operating hours, we assume that the upper bound describes the actual operating hours. Thus, we denote the upper bound of the FLH of a plant technology  $k$  shown in Table B.23 as  $\overline{FLH}_k$  and define the fixed cost of a non-renewable

<sup>19</sup>[https://data.bundesnetzagentur.de/Bundesnetzagentur/SharedDocs/Mediathek/Monitoringberichte/monitoringbericht\\_energie2021.pdf](https://data.bundesnetzagentur.de/Bundesnetzagentur/SharedDocs/Mediathek/Monitoringberichte/monitoringbericht_energie2021.pdf)

generation unit  $s \in S$  as:

$$h_s = \frac{P_s \text{OPEX} x_{k(s)}}{FLH_{k(s)}}$$

where  $k(s)$  denotes the fuel/plant type of generation unit  $s$ . Appendix C describes what non-RES capacities we assume.

### Appendix C. Matching of Generators to Grid Locations

The BZR grid data specify the nominal capacity of thermal generating units at each node, but information on the specific plant type and its operating restrictions are not provided. A different data set provides the aggregate capacity of each specific plant type (e.g., Hard Coal old, Hard Coal new, Gas CCGT, etc.) as well as their operating characteristics (e.g., minimum uptime constraints). Unfortunately, no straightforward mapping exists between the two datasets.

As discussed in Section 2.2, we first identify each thermal unit’s broad plant type (e.g., hard coal, gas, etc.) by matching IDs with the *Kraftwerksliste* (power plant list) provided by the Bundesnetzagentur. Next, we need to distribute these plants to the sub-categories provided in the seller data. For example, all hard coal units must be distributed between Hard Coal old1, Hard Coal old2, and Hard Coal new, with each sub-category having different operational characteristics.

To perform this mapping, we solve an integer program (Schmitt, 2023). Let  $K$  be the set of broad plant types (e.g., hard coal, gas) and  $A_k$  be the set of sub-categories (e.g., Hard Coal old1, Hard Coal old2, Hard Coal new) for each type  $k$ . The total capacity and number of units of each specific plant type  $a \in A_k$  is given as  $P_a$  and  $n_a$  from the seller data. From the grid data, we obtain a set of generators  $I_k$  for each broad plant type  $K$ , each having a nominal capacity of  $p_i, i \in I_k$ . We denote as  $x_{ia} \in \{0, 1\}$  as the desired mapping of each generator to a specific plant type.

With this notation, the mapping problem looks as follows:

$$\begin{aligned} \min_x \quad & \sum_{k \in K, a \in A_k} -n_a(P_a - \sum_{i \in I_k} p_i x_{ia}) + \sum_{k \in K, a \in A_k} -P_a(n_a - \sum_{i \in I_k} x_{ia}) & (C.1) \\ \text{subject to} \quad & \sum_{a \in A_k} x_{ia} = 1 \quad \forall i \in I_k, k \in K \\ & 0 \leq P_a - \sum_{i \in I_k} p_i x_{ia} \leq 600 \quad \forall a \in A_k, k \in K \\ & 0 \leq N_a - \sum_{i \in I_k} x_{ia} \leq 2 \quad \forall a \in A_k, k \in K \end{aligned}$$

The objective function minimizes the aggregate differences in both capacities and number of units per plant type, with equal weight. The first constraint ensures that each unit of broad type  $k$  (e.g., hard coal) is assigned to exactly one specific plant type  $a \in A_k$  (e.g., Hard Coal old1). The last two constraints bound the maximum allowed deviations in capacities and the number of units for each specific plant type  $a$ . Note that a broad type  $k$  could not be identified for all

units, and such unidentified units could be matched freely to any specific type  $a$ . After solving the optimization problem, we obtain a specific type  $a$  for each unit in the grid model and can use its respective operating characteristics as input to the clearing problem in (1).

The result of this mapping is presented in Table C.24. Especially hard coal, lignite, and oil plants could be mapped almost perfectly. Concerning gas units, the grid and seller datasets exhibited more significant differences, which is reflected in the mapping.

Fuel / PlantType	Seller Data		Grid Data	
	Capacity [MW]	Units	Capacity [MW]	Units
Hard Coal / old1	1,905.1	8	1,905	8
Hard Coal / old2	5,172.4	27	5,165.4	27
Hard Coal / new	5,178	8	5,178	7
Lignite / old1	4,989.3	13	4,989	13
Lignite / old2	3,111.1	11	3,111	11
Lignite / new	6,437.8	11	6,437	9
Gas Conventional / old1	776.01	26	775.97	26
Gas Conventional / old2	1215.4	23	1,215.33	23
Gas CCGT / old1	3,601.049	78	3,001.054	78
Gas CCGT / old2	5,356.22	40	5,055.723	38
Gas CCGT / new	7,389.1	45	6,789.321	43
Gas OCGT / old	760.1	15	760.025	15
Gas OCGT / new	2,613.168	66	2,013.224	66
Gas CCGT / present1	64	2	64	2
Gas CCGT / present2	282	2	282	2
Light oil	998.33	21	997.43	21

Table C.24: Generator Mapping Results

## Appendix D. Results for other Redispatch Models

in kEUR	National	2 Zones (k)	2 Zones (s)	3 Zones	4 Zones	Nodal
Generation	33,507.00	33,702.87	33,697.10	33,578.77	33,717.41	36,150.7
RD-Min-Comp	3,567.84	3,421.81	3,457.25	3,546.4	3,449.39	0
Total RD-Min-Comp	37,074.84	37,124.68	37,154.35	37,125.17	37,166.8	36,150.7
RD-Min-Vol	5,736.95	5,506.98	5,598.22	5,694.76	5,560.43	0
Total RD-Min-Vol	39,243.95	39,209.85	39,295.32	39,273.53	39,277.84	36,150.7

Table D.25: Average Daily Costs